Pattern recognition receptor-mediated acquisition of salt stress tolerance in *Arabidopsis thaliana*

Eliza Po-iian Loo
Nara Institute of Science and Technology
Graduate School of Biological Sciences, Laboratory of Plant Immunity
Yusuke Saijo
Submission date 2019/07/26

Graduate School of Biological Sciences Doctoral Thesis Abstract

Laboratory (Supervisor)	Laboratory of Plant Immunity (Yusuke Saijo)		
Name	Eliza Po-iian, Loo	Date	2019/07/26
Title	Pattern recognition receptor-mediated acquisition of salt stress tolerance in *Arabidopsis thaliana*		

In plants, extracellular recognition of immunogenic molecular patterns such as microbe-associated molecular patterns (MAMPs) or plant-derived damage-associated molecular patterns (DAMPs) by cognate pattern recognition receptors (PRRs) leads to an enhanced state of immunity known as pattern-triggered immunity (PTI). Successful pathogens inject specialized proteins and toxins, termed effectors, to dampen PTI. Recognition of effectors by intracellular receptors trigger immune responses that are typically stronger and more robust than PTI, known as effector-triggered immunity (ETI). Some branches of PTI and ETI involve the lipase-like nuclear-cytoplasmic defense regulator EDS1 for signal amplification.

This study reports that, following immunogenic pattern recognition, PRRs also trigger salt stress tolerance in *Arabidopsis thaliana*. Together with the host lab, I show that seedlings pre-treatment with bacterial MAMPs flg22 and elf18 or the DAMPs Pep1-Pep4 induces enhanced salt tolerance in seedlings. Pattern-triggered salt tolerance is impaired in mutant plants defective of PTI signaling, demonstrating the requirement for PTI signaling components in this process. Plants also acquire osmotic stress tolerance after an exposure to mild salt stress, in the absence of exogenous pattern application or microbes. This is accompanied by induction and release of the DAMP precursor PROPEP3 and is dependent on Pep receptors (PEPRs), pointing to intimate functional relationship between PTI and salt stress signaling.

Transcriptome profiling in Pep1-induced salt tolerance reveals an inventory of differentially expressed genes that are sensitized for salt responsiveness in a manner dependent on PEPRs. These genes are over-represented with the WRKY transcription factor binding sites within 1000-bp upstream of the transcriptional start sites. This suggests a possible role for WRKY transcription factors in the regulation of Pep1-induced salt tolerance. With a focus on defense-related WRKY members, I found that WRKY18/WRKY40 act as critical regulators of pattern-triggered salt tolerance, as evident

with a significant decrease in pattern-triggered salt tolerance in *wrky18 wrky40* double

mutant plants. Furthermore, immunoblot analyses indicate that MAMP/DAMP pretreatment increases WRKY18 and WRKY40 protein accumulation under salt stress. A previous study from the host lab reported that activation of EDS1-mediated immunity negatively affects the acquisition of osmotic tolerance following pre-exposure to mild salt stress. This points to apparent discrepancy, in which defense activation through PRRs and EDS1 positively and negatively influences salt/osmotic stress tolerance, respectively. I reconcile this discrepancy with genetic studies on combinations of *wrky18 wrky40* and *eds1* mutant plants, which indicate that PRR signaling leads to salt tolerance in part through WRKY18/WRKY40-mediated attenuation of EDS1 function. This seems to occur at least at the level of *EDS1* expression, since *EDS1* is de-repressed in *wrky18 wrky40* mutant plants during pattern-triggered salt tolerance.

The biological relevance of our findings is strengthened by my finding that inoculation of non-pathogenic bacteria, which activate PRRs, also confers salt tolerance to plants. Importantly, PTI signaling components and WRKY18/WRKY40 are again required for bacterium-induced salt tolerance. I show that heat-killed bacteria also confer salt tolerance, making it most likely that recognition of their MAMPs is sufficient to induce salt tolerance.

In sum, this study provides compelling evidence that MAMP/DAMP recognition leads to salt tolerance by coopting PTI signaling components. Moreover, importantly, it uncovers that MAMP/DAMP-induced involvement of WRKY18/WRKY40 serves to attenuate strong activation of EDS1-dependent defenses, thereby conferring salt tolerance. In addition, my results point to a close functional linkage between the previously described salt tolerance pathway i.e. the salt overly sensitive (SOS) signaling pathway, and PRR signaling pathways. My findings provide genetic evidence for and mechanistic insight into PRR functions in plant adaptation not only to biotic but also abiotic stresses.

TABLE OF CONTENTS

INTRODUCTION

Biotic-abiotic stress signaling crosstalk

Plants in their natural habitats are continuously and often simultaneously challenged with biotic and abiotic stressors. Consequently, they have evolved complex molecular and cellular mechanisms to tolerate not only specific stress but also combinations of stresses (Nejat and Mantri, 2017). Response to one environmental stress could positively or negatively influence another stress response.

In a negative relationship, one stressor penalizes the resistance/tolerance towards another, a phenomenon known as trade-off. For instance, tomato plants under increasing salt stress show more severe disease symptoms with pathogenic fungi *Fusarium oxysporum* (Daami-Remadi et al., 2009). A trade-off is considered as a response to reduce fitness costs since stress responses are energy-consuming processes. On the other hand, in a positive relationship or cross-tolerance, one stressor promotes the tolerance to another, as such, short exposure to high temperature improves Arabidopsis resistance towards *Pseudomonas syringae* pv. tomato DC3000 (*Pst* DC3000; Kusajima et al., 2012). The decision-making mechanisms toward trade-off or cross-tolerance remain largely unknown.

The plant immune system

Plants adopt a unique innate immune system in which each cell is capable of immune signaling upon pathogen challenge (Figure 1; Jones & Dangl, 2006). Each cell carries a repertoire of pattern recognition receptors (PRRs) at the cell surfaces to detect cognate ligands, typically microbial signatures known as microbe-associated molecular patterns (MAMPs) or host-derived damage-associated molecular patterns (DAMPs) released upon cellular damage (Boller and Felix, 2009). MAMPs/DAMPs binding to their cognate PRRs activates cellular signaling that leads to pattern-triggered immunity (PTI). A major class of PRRs is receptor-like kinases (RLKs) that carry an extracellular ligand-binding domain, a transmembrane domain and an intracellular kinase domain (Gust and Felix, 2014; Ma et al., 2016).

In *Arabidopsis thaliana* (*A. thaliana*), the leucine rich repeat (LRR) receptor kinase (RK) FLS2 recognizes a 22-amino-acid epitope of bacterial flagellin known as flg22, whereas the LRR-RK EFR recognizes an 18-amino-acid epitope of bacterial elongation factor-Tu, elf18 (Kunze, 2004; Zipfel et al., 2006). MAMP binding to these receptors recruits the co-receptor LRR-RK BAK1 to form receptor complexes (Chinchilla et al., 2007; Heese et al.,

2007). BAK1 complex formation with PRRs triggers BAK1 phosphorylation that is crucial for PTI signaling. This is indicated in diminished PTI output and increased bacterial pathogen susceptibility in *A. thaliana* mutant plants carrying kinase-inactive BAK1 alleles (Perraki et al., 2018; Schwessinger et al., 2011).

BAK1 and its related SERK family members, including BKK1 contribute to PTI signaling (Roux et al., 2011). However, BAK1 functions in diverse pathways in addition to defense signaling such as brassinosteroid signaling, light responses and cell death control (Saijo et al., 2018). Two *BAK1* mutant alleles, namely *bak1-4* and *bak1-5*, have facilitated the dissection of BAK1 functions in defense signaling. The null mutant, *bak1-4* plants partially retains PTI signaling ability due to genetic redundancy with SERKs, whereas kinase-hypoactive *bak1-5* plants are specifically impaired in PTI signaling without significantly affecting other BAK1-mediated processes (Roux et al., 2011; Schwessinger et al., 2011).

BIK1 and its close homolog PBL1 are among the receptor-like cytoplasmic kinases (RLCKs) that are closely related to RLKs in the kinase domain but lack the extracellular domain. They associate with BAK1 and PRRs in a non-elicited state (Lu et al., 2010; Zhang et al., 2010). Following MAMP perception, PRR-triggered phosphorylation cascade leads to BIK1 activation and dissociation from the receptor complexes to mediate downstream signaling (Lal et al., 2018; Lu et al., 2010; Zhang et al., 2010). BIK1 positively contributes to PTI as seen with decreases in defense outputs and fungal/bacterial resistance of *bik1* mutant plants (Veronese, 2005; Zhang et al., 2010). Following dissociation from the receptor complex, BIK1 phosphorylates and thereby activates the plasma membrane-localized NADPH oxidase RBOHD to promote reactive oxygen species (ROS) production in the apoplast (Kadota et al., 2015; Li et al., 2014; Nühse et al., 2007).

ROS have anti-microbial properties and also serve as important signaling molecules in plant immunity (Kadota et al., 2015). *A. thaliana* carries 10 members of RBOH, of which, RBOHD and RBOHF function redundantly in cell death control and systemic signaling in response to biotic and abiotic stress (Kadota et al., 2015; Miller, 2009; Torres and Dangl, 2005). During PTI, however, RBOHD predominantly mediates ROS production, whereby *rbohd* mutant plants are incapable of inducing a ROS burst following MAMP and pathogen elicitation (Nühse et al., 2007; Torres et al., 2002).

Two major MAPK cascades, namely the MPK3/MPK6 and MPK4 cascades, are activated in defense signaling (Meng and Zhang, 2013). Both MPK3/MPK6 and MPK4 signaling modules are central for signal transduction to activate global transcriptional reprogramming with an array of transcription factors including the WRKY transcription factors (Kushalappa et al., 2016; Yu et al., 2017). The plant-specific WRKY transcription

factor family carry a conserved peptide sequence WRKYGQK, which provides a DNA-binding domain. WRKYs exert their regulatory functions as transcriptional activators or repressors by binding to a DNA sequence (TTGACT/C) known as the W-box (Bakshi and Oelmüller, 2014; Duan et al., 2007; Rushton et al., 2010). Many members of the WRKY family are prominently induced in response to flg22, and they seem to have a role in the regulation of defense genes given the over-representation of W-boxes in the promoters of flg22-inducible genes (Birkenbihl et al., 2016; Navarro, 2004; Zipfel et al., 2004).

Among WRKY transcription factors in *A. thaliana*, WRKY18 and WRKY40 are strongly induced in response to flg22 and redundantly suppress the expression of *EDS1* encoding a defense regulator, thereby attenuating resistance e.g. towards powdery mildew fungi (Birkenbihl et al., 2016; Pandey et al., 2010; Schön et al., 2013). Conversely, however, *wrky18 wrky40* mutant plants show lowered immunity to avirulent *Pst* DC3000 *AvrRps4* that triggers effector-triggered immunity (ETI, see below) via EDS1 (Schön et al., 2013). These studies imply that WRKY18 and WKRY40 play a dual role as negative regulators and positive regulators of EDS1-mediated defense responses in a context dependent manner. Alternatively, not mutually exclusively, WRKY18/WRKY40 contributes to an EDS1-independent step in the latter. Moreover, WRKY18 and WRKY40 have been described to regulate abiotic stress responses as well. For instance, WRKY40 is required for enhanced tolerance to osmotic and salt stress in *wrky18* plants (Chen et al., 2010; Shang et al., 2010). The mechanisms by which WRKY18/WRKY40 regulate defense activation and abiotic stress responses require further studies.

Among the PTI genes directly activated by WRKY18 and WRKY40 are *PROPEP2, PROPEP3* and *PEP RECEPTOR1* (*PEPR1*; Birkenbihl et al., 2016). In *A. thaliana*, some *PROPEPs* are induced in response to MAMPs, pathogen challenge and wounding damage (Huffaker and Ryan, 2007). PROPEPs harbor a short immunogenic Pep epitope and their release (or that of their cleaved products) to the extracellular spaces, where they are recognized by PEPR1 and/or PEPR2 (Hander et al., 2019; Krol et al., 2010; Yamada et al., 2016; Yamaguchi et al., 2006, 2010). Upon Pep perception, PEPRs trigger PTI-characteristic defense responses similar to that triggered by MAMPs (Tintor et al., 2013). In addition to inducing the expression of defense genes, Peps also induce the transcription of their own precursor *PROPEP* genes, thereby forming positive feedback signaling to amplify PTI responses (Huffaker and Ryan, 2007).

Successful bacterial pathogens evade PTI by injecting effectors (proteins and toxins) into the plant cell via a syringe-like structure called the type three secretion system (T3SS). Effectors have specialized functions that enable them to manipulate and overcome PTI responses often by targeting its signaling components (Cunnac et al., 2009; Dodds and

Rathjen, 2010; Xiang et al., 2008; Xin et al., 2018; Zhang et al., 2010). Notably, a bacterial mutant, *Pst* DC3000 *ΔhrpS* that lacks the component required for T3SS function is unable to grow in plant cells (thus, non-pathogenic) due to compromised effector delivery (Dodds and Rathjen, 2010; Xin et al., 2018).

To counter the effectors, host deploys specific intracellular effector recognition receptors known as the nucleotide-binding LRR receptors (NLRs). NLR recognition of effectors leads to effector-triggered immunity (ETI; Boller and Felix, 2009; Jones and Dangl, 2006). The cellular events during and following ETI are largely similar to that of PTI including Ca^{2+} influx, ROS burst, MAPK activation and transcriptional reprogramming (Tsuda and Katagiri, 2010). Despite these similarities, compared to PTI, ETI is typically greater in the amplitude and also more robust against pathogen-mediated perturbations, and are often accompanied by localized cell death called the hypersensitive response (Katagiri and Tsuda, 2010; Tao, 2003). As such, ETI incurs higher fitness costs than PTI does (Katagiri and Tsuda, 2010). It is still largely unexplored whether and how the different layers of immunity influence abiotic stress tolerance and vice versa.

There are two major classes of NLRs classified based on their N-terminal domains, namely the coiled-coil (CC)-NLRs and the Toll-interleukin1-receptor (TIR)-NLRs. CC-NLRs and TIR-NLRs trigger ETI responses predominantly through the central defense regulators NON-RACE SPECIFIC DISEASE RESISTANCE1 (NDR1) and ENHANCED DISEASE SUSCEPTIBILITY1 (EDS1), respectively (Lee and Yeom, 2015; Lukasik and Takken, 2009). Despite such specific assignment of EDS1 and NDR1 to distinct classes of NLRs, the CC-NLR RPS2 recruits EDS1 to confer resistance against *Pst* DC3000 (Bhandari et al., 2019), indicating a cross-regulation. EDS1 also positively regulates basal resistance to invasive biotrophs and hemi-biotrophs (Wiermer et al., 2005).

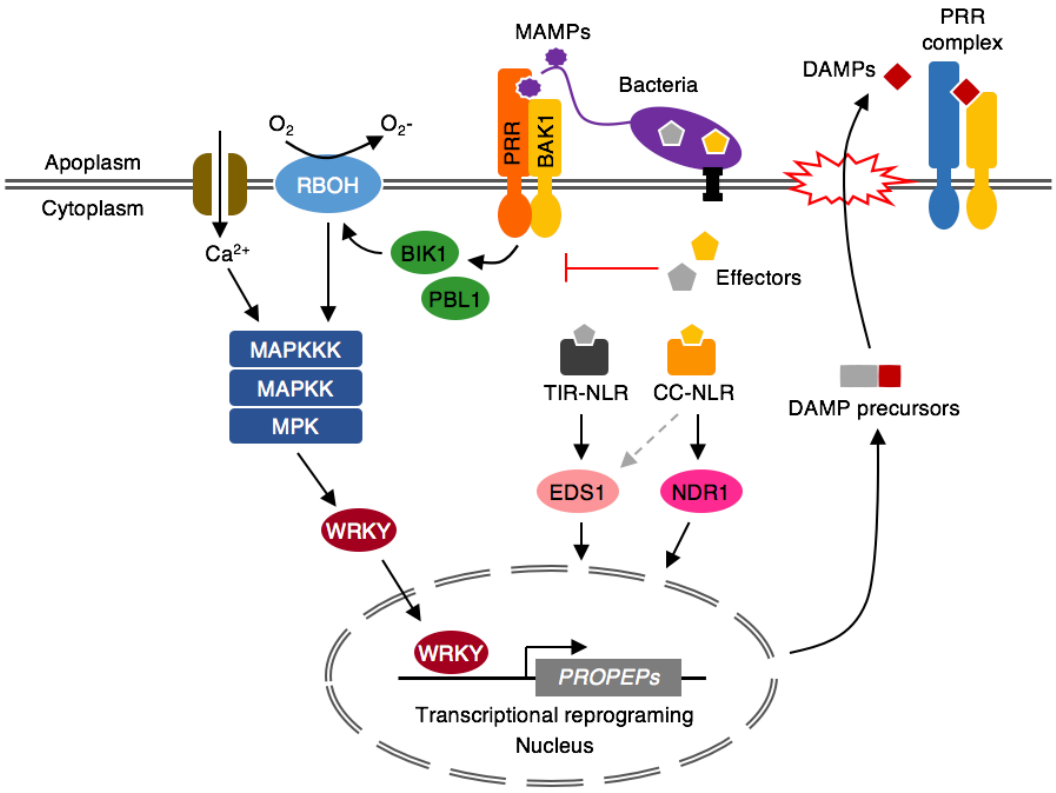

Figure 1: The plant innate immune signaling pathway
MAMPs recognition by PRRs leads to PRR-BAK1 complex formation and the disassociation of BIK1/PBL1 from PRR complex. BIK1/PBL1 triggers intracellular signaling activation such as ROS burst, Ca^{2+} signaling and MAPK cascade, leading to transcriptional reprogramming, to which WRKY transcription factors greatly contribute, during PTI. DAMPs such as Pep peptides (or their precursors) are produced and released for recognition by cognate PRRs, resulting in PTI signal amplification. Pathogen injection of effectors into the plant cell dampens PTI. Plants counter effectors with effector-recognition by NLR proteins leading to ETI. EDS1 is a core defense regulator that controls basal immunity and ETI.

The Salt Overly Sensitive (SOS) signaling in salt stress responses

An early response of salt stress occurs within minutes to hours upon salt exposure where plants experience transient changes in turgor, growth and membrane potential (Schubert, 2014). This is followed by osmotic stress or dehydration where ion accumulation in the roots reduces water uptake (Hütsch et al., 2004). Eventually, ion toxicity occurs when the vacuoles stop sequestering salts, causing a rise of toxic Na^+ concentrations leading to impairment in metabolic and physiological processes (Fortmeier and Schubert, 1995). Thus, maintaining cytoplasmic Na^+ at low concentrations under salt stress is critical for plant growth and development (Zhu, 2003).

The isolation of *salt overly sensitive1* (*sos1*), *sos2* and *sos3* mutant plants that exhibit hypersensitivity towards salt stress, as indicated by severe growth inhibition, revealed the key components mediating salt tolerance in *A. thaliana* (Wu et al., 1996; Zhu, 2000). Although

these *sos* mutants vary in the level of salt sensitivity, the lack of additive hypersensitive effects in *sos1 sos2 sos3* double and triple mutant plants suggest that these three components act in concert to confer salt tolerance (Figure 2; Halfter et al., 2000; Quintero et al., 2002; Zhu, 2000).

To date, the identity of Na^+ sensors or salt stress sensors remains unclear. Salt stress-induces an increase in cytoplasmic Ca^{2+} concentrations, raising the possibility that plants perceive excess salt in the form of Ca^{2+} dishomeostasis (Choi et al., 2014). SOS3 is a Ca^{2+} binding protein that functions as an intracellular Ca^{2+} sensor to perceive Ca^{2+} influx during salt stress (Ji et al., 2013; Liu and Zhu, 1998). A structural analysis on SOS3 protein shows that Ca^{2+} binding triggers conformational and surface property changes for signal transduction (Sánchez-Barrena et al., 2005), but SOS3 appears not to have enzymatic activity, suggesting a requirement for interaction with a partner protein in its function (Ishitani et al., 2000).

Indeed, SOS3 interacts with and activates SOS2 in a Ca^{2+}-dependent manner (Halfter et al., 2000). SOS2 is a Ser/Thr protein kinase with an N-terminal kinase catalytic domain and a C-terminal regulatory domain (Guo et al., 2001). The SOS2 C-terminal domain carries an autoinhibitory domain for the kinase activity, which is relieved through physical interaction with SOS3 (Guo et al., 2004; Halfter et al., 2000). Consistent with this model, removal of the SOS3-binding autoinhibitory domain causes constitutive activation of SOS2 (Guo et al., 2004; Liu et al., 2000).

The SOS2-SOS3 complex targets SOS1 Na^+/H^+ antiporter (Ishitani et al., 2000; Shi et al., 2000). Transcriptional gene activation and the antiporter activity of SOS1 during salt stress are controlled by SOS2 and SOS3 (Qiu et al., 2002; Shi et al., 2000). Over-expressing *SOS1*, *SOS2* and *SOS3* in a yeast system revealed that SOS3 recruits SOS2 to the plasma membrane wherein SOS2 phosphorylates and activates SOS1 to drive Na^+ exclusion from the cell (Quintero et al., 2002). Collectively, these studies illustrate the mode of SOS signaling: Ca^{2+} elevation during salt stress is sensed by SOS3, which then physically interacts with and relieves SOS2 from autoinhibition. The complex localizes to the plasma membrane to activate the antiporter activity of SOS1. Moreover, recent studies have revealed novel components mediating osmotic- and ionic-stress-induced gating of Ca^{2+} influx channels (Jiang et al., 2019; Yuan et al., 2014). Whether and if so how they influence SOS signaling and also perhaps other stress responses represent an interesting open question.

The regulatory mechanisms of Na^+ flux and ion homeostasis are more complex than a linear SOS3-SOS2-SOS1 signaling pathway (Figure 2). Studies reported branching of the SOS signaling whereby Na^+-induced activation of SOS1 can occur independently of SOS3-SOS2 complex (Shabala et al., 2005; Yu et al., 2010). This is seen when salt-induced

accumulation of phosphatidic acid drives its binding to MPK6 to trigger the activation of SOS1 (Yu et al., 2010). Additionally, SOS2 also interacts with ABI2, a negative regulator of abscisic acid (ABA) signaling, and disruption of the interaction results in increased salt tolerance (Merlot et al., 2011; Ohta et al., 2003).

The phytohormone ABA plays pivotal roles in abiotic stress regulation, in particular, under water-deficit and osmotic stress conditions (Raghavendra et al., 2010). ABA biosynthesis involves a complex multistep pathway, but the loss of ABA2 function in *aba2* mutant plant was sufficient to significantly lower the biosynthesis and contents, resulting in ABA deficiency (González-Guzmán et al., 2002; Léon-Kloosterziel et al., 1996). A large number of ABA-responsive genes are regulated by the ABA RESPONSIVE ELEMENT BINDING FACTOR (AREB/ABF) transcription factor family (Busk et al., 1997; Choi et al., 2000). Notably, AREB1/ABF2, AREB2/ABF4 and ABF3 act as master transcription factors in ABA signaling under water-deficit stress (Fujita et al., 2005; Furihata et al., 2006; Yoshida et al., 2015). Their significance in drought tolerance is evident with decreased sensitivity to ABA is associated with drought sensitivity in *areb1 areb2 abf3* triple mutant plants (Fujita et al., 2011).

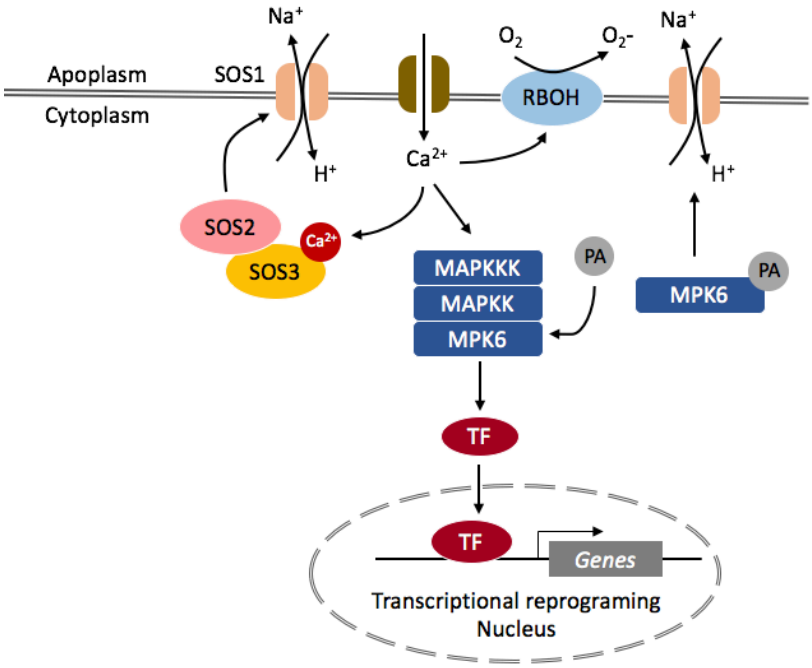

Figure 2: The SOS signaling pathway
Salt stress induces an increase in cytoplasmic Ca^{2+} concentrations that is sensed by the Ca^{2+}-binding protein SOS3. SOS3 interacts with the protein kinase SOS2 to form a signaling complex at the plasma membranes to activate the Na^+/H^+ antiporter SOS1. Activated SOS1 drives a Na^+ efflux to restore the cellular Na^+ homeostasis. In parallel, salt-induced phosphatidic acid (PA) accumulation facilitates MPK6-mediated activation of SOS1.

Signal integration in PTI and salt stress signaling

Components involved in defense responses have been reported to contribute to salt stress tolerance as well. For instance, the expression of *SlWRKY8* in tomato is upregulated in response to both *Pst* DC3000 challenge and salt stress. Transgenic plants overexpressing *SlWRKY8* are more resistant to pathogen *Pst* DC3000 and more tolerant to drought and salt stress (Gao et al., 2019). Furthermore, in *A. thaliana,* RBOHD and RBOHF are also responsible for ROS production in response to salt stress, which is crucial for regulating Na^+/K^+ homeostasis to confer salt tolerance (Jiang et al., 2012; Ma et al., 2012). The intertwined web of PTI signaling presents many possible convergence points for biotic and abiotic stress signaling.

In parallel with my studies, other studies have reported that PRRs are coopted in salt stress tolerance as well. *A. thaliana* plants lacking CERK1, which recognizes a fungal MAMP chitin and mediates perception of bacterial peptidoglycans, are compromised in PTI responses (MAPK and ROS burst activation) and more susceptible to necrotrophic fungi (Miya et al., 2007). Intriguingly, *cerk1* plants are also hypersensitive to salt stress, as indicated by decreased germination and chlorophyll content under salt stress (Espinoza et al., 2017). Accordingly, *A. thaliana* overexpressing fungal endochitinase *chit36* showed increased tolerance to salt in a manner dependent on CERK1 (Brotman et al., 2012). CERK1 interacts with the Ca^{2+} channel ANNEXIN1, which drives salt-induced Ca^{2+} influx and transcriptional activation of *SOS1*, although the significance of ANNEXIN1 is not shown (Davies, 2014). Importantly, these studies suggest the involvement of CERK1 in salt stress adaptation in the absence of microbes, and the shared use of molecular components between chitin-triggered defense and salt stress signaling. However, the mechanisms underlying salt tolerance downstream of CERK1 or the possible involvement of different PRRs remains unexplored in salt tolerance.

Plant cell wall undergoes softening and lowers its integrity under salt stress (Feng et al., 2018). The plasma membrane-localized RLK FERONIA (FER) identifies a cell wall integrity sensor, which may be involved in sensing salt stress damage (Feng et al., 2018). FER recognizes the DAMPs RAPID ALKALIZATION FACTORs (RALFs), including RALF22 and RALF23 that are involved in salt stress and PTI responses (Feng et al., 2018; Stegmann et al., 2017; Xiao et al., 2019). In *A. thaliana,* the loss of FER (*fer*) and overexpressing *RALF22*/*RALF23* both result in salt hypersensitivity (Feng et al., 2018; Zhao et al., 2018). Similarly, in *fer* mutant plants and plants over-expressing *RALF23*, PTI responses and *Pst* DC3000 resistance are also compromised (Stegmann et al., 2017; Xiao et al., 2019). These studies demonstrate the engagement of the RALF22/RALF23-FER in the negative regulation of PTI and salt stress tolerance, providing a common node between PTI and salt signaling pathways.

In *A. thaliana*, application of the DAMP *At*Pep3 and overexpressing *AtPEP3* both enhance salt tolerance in a manner dependent on PEPR1 (Nakaminami et al., 2018). Accordingly, the functional *At*Pep3 region required for induced salt tolerance overlaps with the region that elicits defense responses (Nakaminami et al., 2018). However, the signaling mechanism downstream of the receptor remains totally unclear. Another DAMP in tomato, systemin, is induced under salt stress and overexpression of which confers salt tolerance (Orsini et al., 2009). Also, the extracellular ATPs (eATPs) have been shown to regulate water homeostasis to limit water loss (Chen et al., 2017; Tanaka et al., 2014). Collectively, these studies show that DAMP recognition and signaling play a role in salt stress signaling, but the underlying mechanisms remain to be elucidated.

Aims of this study

Recent studies (in parallel with my study) have pointed to a role for DAMPs and/or PRRs in salt stress responses and/or tolerance, but little information is available for the components downstream of the receptors or their mechanistic bases. The molecular links between defense signaling and salt stress signaling also remain largely unknown.

With the basis on my own findings that PRR activation following MAMP/DAMP application leads to salt tolerance in *A. thaliana* seedlings, this study aims to elucidate the genetic framework and gain mechanistic insight into PRR-mediated salt tolerance (hereafter called pattern-triggered salt tolerance, PTST). This study defines the signaling components involved in PRR-mediated salt stress tolerance. With successful identification of key components regulating PTST, I have attempted to investigate into the mechanisms that link PRR activation to salt stress tolerance. I have further tested the possible divergence between PTI and ETI pathways in the acquisition of salt stress tolerance. Finally, this work examines whether non-pathogenic microbes and their recognition also confer salt tolerance, with attention to the functional and biological relevance of PTST.

MATERIALS AND METHODS

Plant materials and growth conditions

The *Arabidopsis thaliana* accession Col-0 was used as the wild type (WT). Seeds were sterilized with 6% sodium hypochlorite and 0.1% Triton X-10 for 15 minutes, rinsed 5 times with autoclaved distilled water and stratified at 4˚C for 2-5 days before they were grown in Skoog-Murashige (MS) medium (1/2 strength MS basal salts, 25 mM sucrose, 0.5 g/L MES, pH 5.7) under 14 h light/ 10 h dark at 22˚C unless otherwise stated. Plant materials used are as listed in table below.

Genotype	Background	References
WT	Col-0	
pepr1-1 (SALK_059281) *pepr2*-3 (SALK_098161)	Col-0	Tintor et al., 2013
fls2 efr	Col-0	Nekrasov et al., 2009
bak1-4	Col-0	Chinchilla et al., 2007
bak1-5	Col-0	Gonzalez-Guzman et al., 2002
p35S::PEPR1-FLAG	Col-0	Ross et al., 2014
p35S::PEPR2-FLAG	Col-0	Ross et al., 2014
pPROPEP3::PROPEP3-VENUS	Col-0	Ross et al., 2014
wrky18-1 (Gabi_Kat 328G03), *wrky40* (SLAT dSpm)	Col-0	Shen et al., 2007
wrky18-1 (SALK_093916)	Col-0	Xu et al., 2006
wrky40 (SLAT dSpm)	Col-0	Xu et al., 2006
wrky60-1 (SALK_120706)	Col-0	Xu et al., 2006
areb1 areb 2 abf3	Col-0	Yoshida et al., 2010
eds1-2	Col-0	Bartsch et al., 2006
wrky18-1 (Gabi_Kat 328G03), *wrky40* (SLAT dSpm), *eds1-2*	Col-0	Schön et al., 2013
bak1-5 bkk1-1	Col-0	Yamada et al., 2016
rbohD-3 (NASC code N9555)	Col-0	Torres et al., 2002
aba2-12	Col-0	González-Guzmán et al., 2002
wrky33 (GABI_324B11)	Col-0	Logemann et al., 2006
sos2 (SALK_056101C)	Col-0	Alonso et al., 2003
sos3 (SALK_207663C)	Col-0	Alonso et al., 2013
camta3-D	Col-0	Jacob et al., 2018

Pattern-triggered salt tolerance assay

Four-day-old seedlings grown in liquid growth media were treated with the indicated elicitor for 4 days before they were transferred to agar growth media supplemented with 175 mM

NaCl. Seedlings were grown under the normal growth conditions described above, and the number of viable seedlings was scored every day for the indicated duration. Survival percentage is the percentage ratio of the number of viable seedlings on the indicated day to the total number of seedlings used in the assay. Elicitors used are listed in the table below.

Elicitor	Concentration	Manufacturer
flg22	0.1 μM	PepMic Co. Ltd. (China)
elf18	0.1 μM	PepMic Co. Ltd. (China)
Pep1-Pep4	0.1 μM	PepMic Co. Ltd. (China)

Oxidative burst (ROS) assay

The generation of ROS was measured by a luminol-based assay on leaf discs from 4-week-old plants. Leaf discs (5 mm in diameter) were incubated overnight in distilled water in a petri dish. Each leaf disc was then carefully transferred into individual wells with 100 μL of a ROS assay buffer (500 μM luminol, 10 μg/ml horseradish peroxidase) in a 96-well plate and incubated for 5 hours in darkness. Luminescence was measured immediately every 3 minutes for 1 hour after elicitation with 0.1 μM of flg22, with TriStar2 Multimode Reader LB942 (Berthold Technologies).

Acquired osmotic tolerance assay

Seven days-old seedlings grown on agar growth media were transferred to fresh agar growth media supplemented with 100 mM NaCl and further incubated for 7 days. Following 7-day incubation, seedlings were transferred to agar growth media supplemented with 750 mM sorbitol and grown for another 14 days. Chlorophyll content was determined as described in Ariga et al. (2017). Assay was conducted by our collaborator in NODAI Genome Research Center, Tokyo University of Agriculture.

Detection of extracellular PROPEP3-VENUS protein

For Pep1- and salt-treated samples, 14 days-old seedlings in liquid media were exposed to either 0.5 μM Pep1 or 150 mM NaCl, respectively for 3 days under standard growth conditions. For the combination of Pep1 and salt treatments, seedlings were exposed to 0.5 μM Pep1 for 12 hours followed by 150 mM NaCl for 3 days under standard growth conditions. The liquid media were harvested as extracellular fractions for immunoblot analysis. This analysis was conducted with the aid of Dr. Taishi Hirase at the host lab.

Protein extraction and immunoblot analysis

Protein extracts were prepared by homogenizing frozen tissues in a lysis buffer [50 mM Tris-HCl pH7.5, 2% SDS, 2mM DTT, 2.5 mM NaF, P9599 protease inhibitor cocktail (Sigma)] and incubated at room temperature for 15 minutes. The supernatants recovered after centrifugation at 13,000 g for 15 minutes were incubated with the SDS sample buffer at 95°C

for 5 minutes and then subjected to immunoblot analysis on 10% SDS-PAGE with antibodies as listed in table below. Molecular weight markers used was Protein Ladder One (Triple-color; Nacalai Tesque, Japan).

Protein	Primary Antibody	Manufacturer
WRKY18-HA	Anti-HA-Peroxidase 3F10	Roche
WRKY40-HA	Anti-HA-Peroxidase 3F10	Roche
pMAPK	Phospho-p44/42 MAPK (Erk1/2) (Thr202/Tyr204)	Cell Signaling Technology
PROPEP3-VENUS	Anti-PROPEP3 (Ross et al., 2014)	-

RNA sequencing and analysis

Plant materials were grown as described above. Three biological replicates were prepared for each treatment in which total RNA was extracted with a commercial kit (NucleoSpin RNA, Machery-Nagel). Library preparation, high-throughput sequencing and library quality check was conducted with paired-end, 100-bp deep sequencing on an Illumina HiSeq (HiSeq2500) platform by collaborators at the Cooperative Research Grant of the Genome Research for BioResource, NODAI Genome Research Center, Tokyo University of Agriculture. Reads were mapped to the TAIR9 Arabidopsis transcriptome database (https://www.arabidopsis.org). The edgeR software package (bioconductor.org.packages/release/bioc/html/edgeR.html) was used for estimation of false discovery rate (FDR) for differential gene expression of raw reads from all 3 biological replicates of each treatment. Heat map was generated with an R-software heat map tool from gplot package (https://cran.r-project.org/web/packages/gplots/) with differentially expressed genes (DEGs) identified using the following cut-off values: FDR <0.05, expression $|\log_2 FC \geq 1|$ and Student t-test $p < 0.05$. Gene read counts were normalized to RPKM values and hierarchical clustering was conducted with one minus Pearson correlation complete linkage.

***In silico* transcription factor binding site analysis**

Sequences 1000 bp upstream of the annotated transcriptional start sites of genes of interest were examined with the MEME suite 5.0.5 online tool (http://meme-suite.org). Motif enrichment was performed with Local Motif Enrichment Analysis CentriMo with reference to DAP motifs (O'Malley 2016) ARABIDOPSIS (*Arabidopsis thaliana*) DNA database. Analysis was performed only on the given (sense) strand with *E*-value threshold for enriched regions of less than 0.00001.

Quantitative RT-PCR analysis

Total RNA was extracted from plant samples with Purelink (Nacalai Tesque, Japan) and reverse transcribed with PrimeScript Reagent Kit Perfect Real Time (Takara, Japan) according to manufacturer's instructions. qRT-PCR was performed with Power SYBR Green PCR Master Mix (Applied Biosystems, Japan) using the Thermal Cycler Dice RealTime TP870 (Takara, Japan) under the following conditions: 50°C 2 min, 95°C 10 min, 95°C 15 s

followed by 60°C 1 min for 40 cycles, then 95°C 15 s, 60°C 30 s, and finally 95°C 15 s. Primers pairs used are as listed in the table below.

Gene	Forward primer	Reverse Primer
EDS1	CCAGCGATGAACAAGAATGGTCTC	TGAACGTACTGTCTGCCTCTTGTGC
Actin2	ACCTTGCTGGACGTGACCTTACTGAT	GTTGTCTCGTGGATTCCAGCAGCTT
PTR3	CATTTTCTTGTTGGGCACTCCGTTT	TGGGATGCTGAAAGATCCGGTAAC

Bacteria inoculation for salt tolerance assay

Pseudomonas syringae DC3000 *ΔhrpS, AvrRpm1, AvrRps4* and *Pseudomonas fluorescens* were grown in NYGB (5 g/L peptone, 3 g/L yeast extract, 20 mL/L glycerol, pH7.0) supplemented with appropriate antibiotics (rifampicin 25 mg/mL in DMSO, kanamycin 50 mg/mL in ddH_2O, tetracyclin 15 mg/L in ethanol, chloramphenicol 30 mg/mL in ethanol). Cultivation was performed overnight (~16 hours) at 28°C with 200 rpm shaking incubation. Overnight cultures were washed at least twice with 10 mM $MgCl_2$ and the titer was adjusted to OD_{590} = 0.002 for spray inoculation. Seedlings were transferred from liquid media to agar plates 1 day prior to spray-inoculation. Inoculated seedlings were incubated in the growth chamber for 6 hours before they were surface sterilized twice with 70% ethanol followed by rinsing twice with autoclaved ddH_2O. Seedlings were then transferred to fresh agar media supplemented with 175 mM NaCl.

RESULTS

Damage/Microbe-associated molecular patterns trigger salt tolerance

An *in silico* analysis for the previously described transcriptome data for elf18-/Pep2-inducible genes in their salt stress responsiveness points to a substantial overlap between PTI and salt stress responses (Figure 3). Close inspection revealed that components of PEPR signaling that were highly induced during defense signaling, i.e. *PROPEP1-PROPEP3, PEPR1* and *PEPR2*, were more highly induced under salt stress than defense non-inducible components of PEPR signaling such as *PROPEP5* and *PROPEP6* (Bartels et al., 2013). This prompted the host lab and me to test whether, and if so, how MAMP and DAMP signaling pathways play a role in salt stress response.

To this end, I have developed an assay to assess the effects of MAMP/DAMP application on the tolerance of *A. thaliana* seedlings under salt stress. In this assay, seedlings pre-treated with MAMPs/DAMPs of interest under sterile conditions are subjected to salt stress. The degree of salt tolerance was quantified at the tested time points by calculating the ratio between the numbers of viable seedlings therein and the total number of seedlings tested. Remarkably, seedlings pre-treated with Pep2 displayed a significantly increase in the tolerance to salt stress, as indicated by the retention of higher number of green plants (Figure 4A). By contrast, a much greater ratio of mock-treated seedlings showed leaf bleaching, indicating seedling death. Importantly, the Pep2 effects were not seen in *pepr1 pepr2* seedlings, validating that Pep2 pre-treatment enhances salt tolerance of seedlings in a manner dependent on the cognate receptors PEPR1/PEPR2.

I further tested whether different DAMPs and MAMPs also confer salt tolerance. As described, seedlings were treated with other Pep family members, including Pep1, Pep3 and Pep4, and the MAMPs flg22 and elf18 prior to salt stress. While only about 20% of mock-treated wild-type (WT) seedlings survived after 7 days of salt exposure, Pep1, flg22 and elf18 pre-treatment remarkably improved salt tolerance, allowing more than 80% of the seedlings to survive the given salt stress (Figure 4B). Pre-treatment with all the MAMPs and DAMPs tested rescued at least 65% of seedlings under salt stress, in the presence of their cognate PRRs (Figure 4B, Table 1).

I also tested whether salt tolerance is conferred by the fungal MAMP chitin, which triggers PTI via CERK1 (Cao et al., 2014). Under our conditions, pre-treatment with chitin did not confer PTST (Figure 5A). To ensure the effectiveness of the chitin elicitor used in immune activation, I examined the expression of a previously described chitin-inducible gene,

CYP71A13 (Zhang et al., 2013). Chitin elicitation of *A. thaliana* seedlings for 1 hour successfully induced the expression of *CYP71A13* (Figure 5B), validating my conclusion stated above.

Pep1 pre-treatment induced salt tolerance in *pepr1* and *pepr2* single mutant plants, indicating that either PEPR1 or PEPR2 is sufficient to confer salt tolerance as described previously for immune activation (Table 1; Yamaguchi et al., 2010). The ability of different MAMPs and DAMPs to induce salt tolerance indicates that this phenomenon is not unique to particular MAMP/DAMP or PRR, but common to a broad range of MAMPs/DAMPs, hence designated pattern-triggered salt tolerance (PTST). Since Pep1 pre-treatment consistently shows the greatest increase in salt tolerance, I used Pep1 for subsequent analyses, unless otherwise stated.

Next, dose dependence was determined for PTST. The magnitude of salt tolerance appeared to be dose-dependent whereby 0.01 μM of flg22 was sufficient to establish PTST at apparently saturated levels (Figure 4C). This concentration is comparable with the previously described concentrations of MAMPs/DAMPs required to elicit PTI responses (Aslam et al., 2009), which is compatible with the notion that PTST and PTI share common mechanisms. The minimum dose requirement also agreed with the concentration previously described for *At*Pep3-induced salt tolerance (Nakaminami et al., 2018). The number of survivors was not further increased from 0.1 μM to 0.5 μM flg22 pre-treatments, implying that flg22 was saturated at 0.1 μM. Thus, 0.1 μM has been selected for subsequent analyses.

Of note, PTI activation in response to Pep1 and flg22 typically results in plant growth inhibition (Gomez-Gomez et al., 1999; Krol et al., 2010). To test whether root growth retardation is required for PTST, the root length of WT seedlings following Pep1, Pep3, and Pep4 treatment was determined. Compared to the mock control, Pep1 treatment inhibited root growth by 2-fold in WT seedlings, whereas Pep3 and Pep4 treatments did not have significant effects on root growth (Figure 4D). Notably, however, Pep1, Pep3 and Pep4 were largely indistinguishable in conferring PTST (Table 1). Thus, Pep1-induced root growth inhibition is not required for PTST.

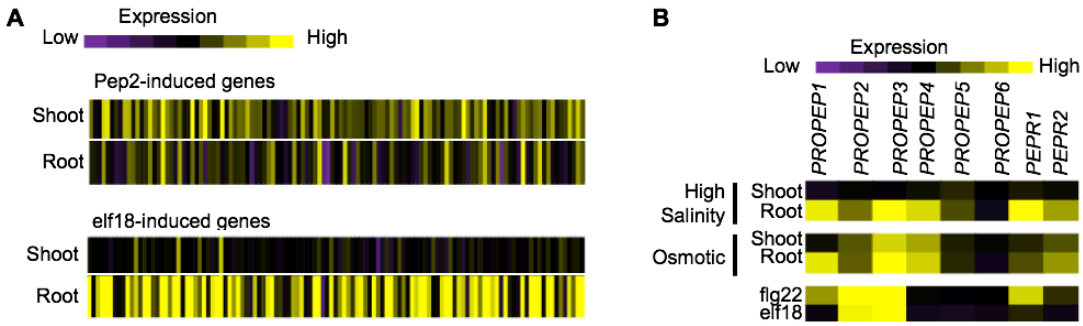

Figure 3: Over-representation of salt-inducible genes in PTI-inducible genes Heat maps summarizing the *in silico* gene expression analysis of (A) salt-responsiveness in the top 1000 Pep2- and elf18-inducible genes in the roots and shoots of *A. thaliana* and (B) responsiveness of *PROPEPs* and *PEPRs* with salt, osmotic stress and MAMPs elicitation.

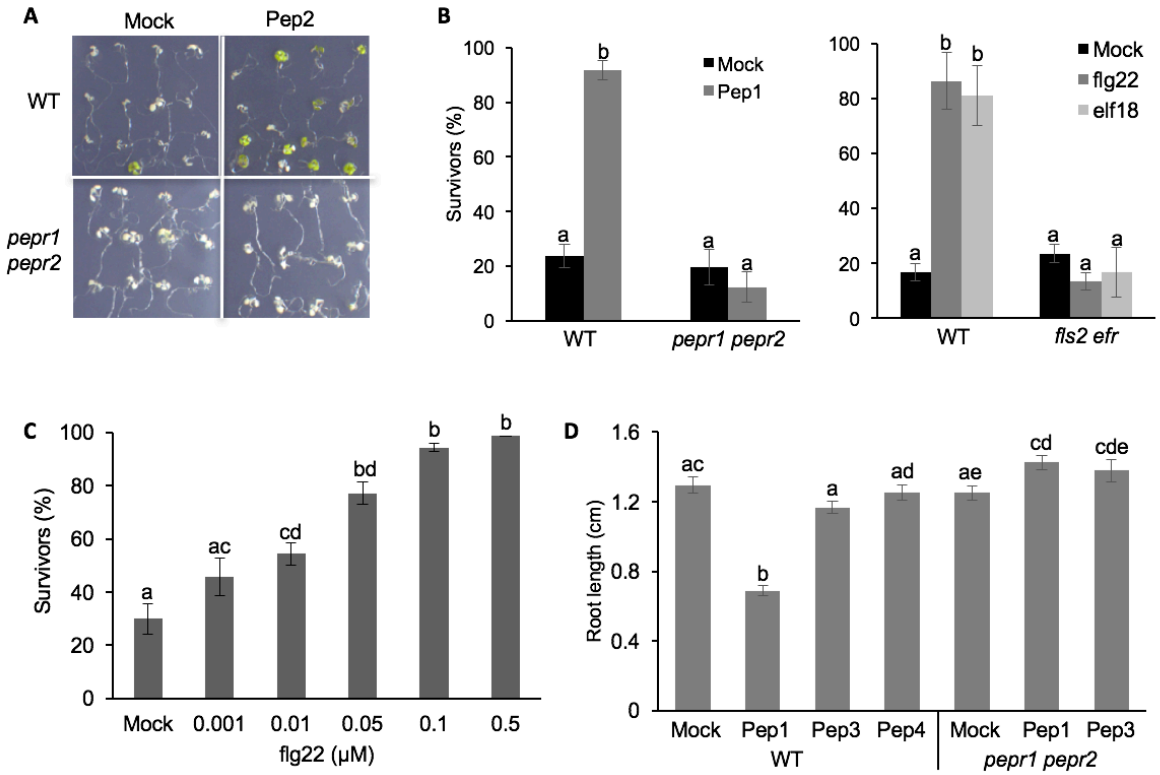

Figure 4: MAMP/DAMP pre-treatment in *A. thaliana* seedlings enhances salt tolerance

A. Representative phenotypes of the 14-day-old WT and *pepr1 pepr2* seedlings, with and without 0.1 μM Pep2 pre-treatment, 6 days after exposure to 150 mM NaCl.

B. Survival rate (%) of WT and PRR mutants, with and without 0.1 μM MAMP/DAMP pre-treatment, 7 days after exposure to 175 mM NaCl. Data from at least two independent experiments (N >60), error bars indicate standard error. Letters above bars indicate p <0.05 calculated using Tukey's HSD.

C. Survival rate (%) of mock and 0.001 μM to 0.5 μM of flg22 pre-treated WT seedlings, 7 days after exposure to 175 mM NaCl. Data from at least two independent experiments (N >60) are shown. Error bars indicate standard error. Letters above bars indicate p <0.05 calculated with Tukey's HSD.

D. Root lengths of WT and *pepr1 pepr2* seedlings, 4 days post 0.1 μM of Pep1, Pep3 or Pep4 treatment. Data from the average of at least 30 seedlings. Error bars indicate standard error. Letters above bars indicate p <0.05 calculated with Tukey's HSD.

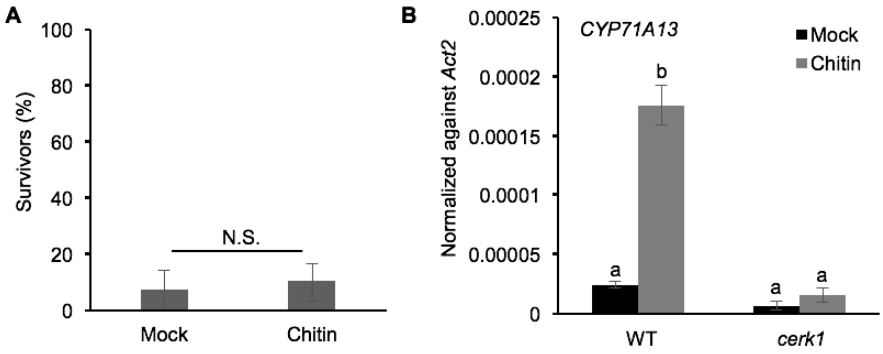

Figure 5: Chitin does not confer PTST

A. Survival rate (%) of WT seedlings, with and without 100 μg/ml chitin pre-treatment, 7 days after exposure to 175 mM NaCl. Data from at least 2 independent experiments (N >60), error bars indicate standard error. N.S.- not significant calculated using two-tail t-test.

B. qRT-PCR analysis on the expression of *CYP71A13* in 7-day-old WT and *cerk1* seedlings treated with 100 μg/ml chitin for 1 hour. A representative figure from 2 independent experiments is shown. Error bars indicate standard error. Letters above error bars indicate $p < 0.05$ calculated using Tukey's HSD.

Table 1: PEPR1 and PEPR2 both contribute to *At*Pep-induced salt tolerance in *A. thaliana* seedlings. Survival rate (%) of each genotype tested, 7 days after exposure to 175 mM NaCl.

Genotype	Pre-treatment	Survivors/Total seedlings	% Survivors
WT	Mock	5/30	16.6
	Pep1	29/30	96.7
	Pep3	30/46	65.2
	Pep4	40/50	80.0
pepr1	Mock	5/35	14.3
	Pep1	26/30	86.7
pepr2	Mock	1/30	3.3
	Pep1	30/30	100

Pattern-triggered salt tolerance requires previously described PTI signaling components

I next assessed whether the authentic PTI signaling components are required for PTST, by testing its possible alterations in previously described PTI signaling mutants such as *bak1-4, bak1-5, bik1 pbl1*, and *rbohd*.

PRRs have different association preference with BAK1 and related SERK family members in PTI signaling. Notably, EFR and PEPR1/2 are less stringent in their requirement for BAK1 and can mount PTI with other SERK family members, thus retaining recognizable PTI responses in the null *bak1-4* mutant (Roux et al., 2011). On the contrary, FLS2 has a high preference for BAK1 and its signaling function is severely compromised in *bak1-4* plants (Roux et al., 2011). However, these BAK1-associated PRRs are all impaired in *bak1-5* plants, in which a substitution in the cytoplasmic kinase domain dramatically reduces kinase activity and specifically disables PTI signaling function of BAK1(Schwessinger et al., 2011). Therefore, the *bak1-5* allele provides a useful tool to assess the requirements for PTI-related SERK functions in the processes of interest.

Although Pep1-induced salt tolerance was largely retained in *bak1-4* plants, it is impaired in *bak1-5* plants (Figure 6A), as previously described for Pep2-induced immune responses (Yamada et al., 2016). This indicates that BAK1 (or related SERKs) is required for PTST as well as for PTI in the PEPR pathway. Pep1 pre-treatment failed to confer PTST in *bik1 pbl1* mutant plants, while in contrast flg22 pre-treatment successfully conferred PTST (Figure 6C). The differential requirements for BAK1 and BIK1 were reminiscent of that in PTI where PEPRs and FLS2 strictly require BIK1/PBL1 and BAK1, respectively, in PTI (Ranf et al., 2014; Yamada et al., 2016). This strengthens the specific need for the authentic receptor complexes in PTST, in a manner largely indistinguishable from that in PTI.

PTST was not fully compromised but significantly attenuated in *rbohd* plants compared to WT plants (Figure 6B). This is consistent with partially compromised PTI responses in *rbohd* plants, possibly due to functional redundancy with RBOHF (Torres et al., 2002). Collectively, these observations indicate a critical role for the authentic PTI signaling components in both PTI and PTST.

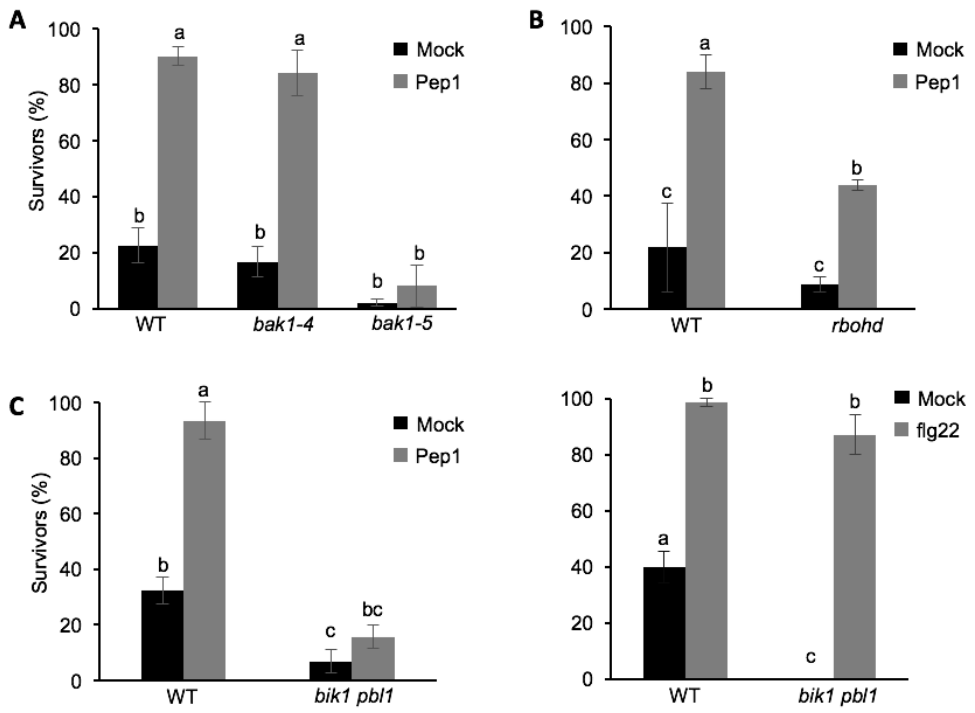

Figure 6: PTST requires authentic PRR complexes and intact PTI signaling pathway

A,B. Survival rate (%) of WT and PTI signaling component mutants, (A) *bak1-4* and *bak1-5,* and (B) *rbohd* mutant seedlings, with and without 0.1 μM Pep1 pre-treatment, 9 days (*bak1-4, bak1-5*) and 8 days (*rbohd*) after exposure to 175 mM NaCl. Data from at least two independent experiments (N >60), error bars indicate standard error. Letters above bars indicate p <0.05 calculated with Tukey's HSD.

C. Survival rate (%) of WT and *bik1 pbl1* double mutant seedlings, with and without 0.1 μM Pep1 or flg22 pre-treatment, 5 days after exposure to 175 mM NaCl. Data from at least two independent experiments (N >60), error bars indicate standard error. Letters above bars indicate p <0.05 calculated with Tukey's HSD.

Pattern-triggered salt tolerance requires SOS signaling but not ABA signaling

Since the SOS signaling pathway plays a major role in salt stress responses, I investigated the possible role of SOS signaling in PTST. To this end, *sos2* and *sos3* mutant plants were tested for PTST. Interestingly, *sos2* and *sos3* plants both failed to confer PTST, pointing to their requirements for PTST (Figure 7A).

As a first step to elucidate how SOS2 and SOS3 contribute to PTST, I next tested whether *sos2* and sos3 plants display possible alterations in different PTI signaling outputs, such as a ROS burst and MAPK activation following flg22 application. Both *sos* mutants retained a ROS burst and MAPK activation at WT-like levels (Figure 7B-C). These observations indicate that these early PTI signaling outputs can be uncoupled from PTST in *sos2* and *sos3* plants, and that they are not sufficient to confer PTST. However, it should be taken into consideration that *sos2* and *sos3* plants could be impaired in PTI signaling under salt stress due to their high sensitivity to salt.

Thus, to assess precisely the possible involvement of SOS2/SOS3 in PRR signaling toward PTST, I tested MAPK activation under PTST conditions, i.e. when subjected to salt stress after their pre-exposure to flg22. Notably, WT plants sustained MAPK activation 4 days after flg22 treatment prior to salt exposure (0 hour). By contrast, *sos2* and *sos3* plants were severely reduced in MPK6 activation not only after but also before the onset of salt stress (Figure 7D). These results for the first time reveal a salt-independent role for SOS2/SOS3 in sustaining MAMP-induced MAPK activation, which seems to facilitate subsequent activation under salt stress. Collectively, these observations suggest that SOS signaling serves to sustain PRR signaling toward PTST.

The importance of ABA has been well documented in osmotic and salt stress signaling. To determine whether ABA is crucial for PTST, I tested possible alterations in PTST in an ABA biosynthesis mutant *aba2-12* and an ABA transcription factors triple mutant *areb1 areb2 abf3*. PTST was retained in both mutants (Figure 8), indicating that ABA is dispensable for PTST.

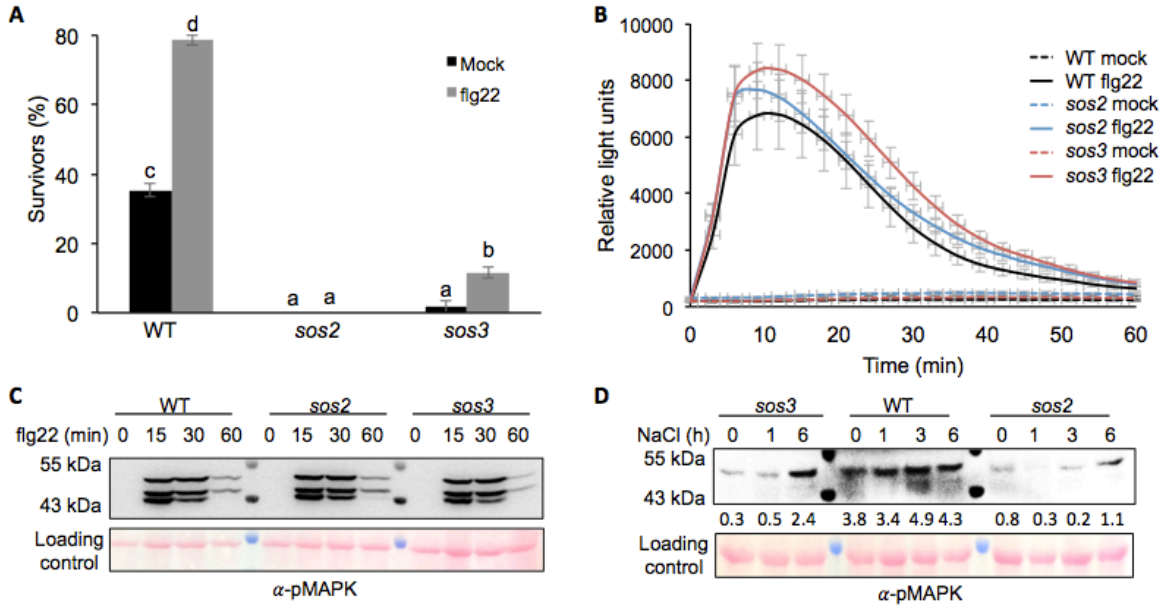

Figure 7: PTST requires components from the SOS signaling pathway

A. Survival rate (%) of WT and SOS mutants, with and without 0.1 μM flg22 pre-treatment, 7 days after exposure to 175 mM NaCl. Data from at least two independent experiments (N >60), error bars indicate standard error. Letters above bars indicate p <0.05 calculated using Tukey's HSD.

B. flg22-induced ROS burst production in WT and SOS mutants. Luminescence of leaf discs from at least 6 leaves of 4-week-old plants, with and without 0.1 μM flg22 treatment. Representative data from at least two independent experiments. Error bars indicate standard error.

C. PTI activation of MAPK in 9-day-old WT and *sos* mutants. Anti-pMAPK immunoblot analysis of seedling treated with 0.1 μM flg22 for indicated period. Representative figure from 3 independent experiments.

D. PTST activation of MAPK in 9-day-old WT and *sos* mutants. Anti-pMAPK immunoblot analysis of seedlings pre-treated with 0.1 μM flg22 for 4 days followed by the indicated period of exposure to 175 mM NaCl. Representative figure from 3 independent experiments. Numbers between blots indicate intensity of each band relative to loading control. According to the molecular weight, the MAPK band seems to correspond to MPK6 (Saijo et al., 2009).

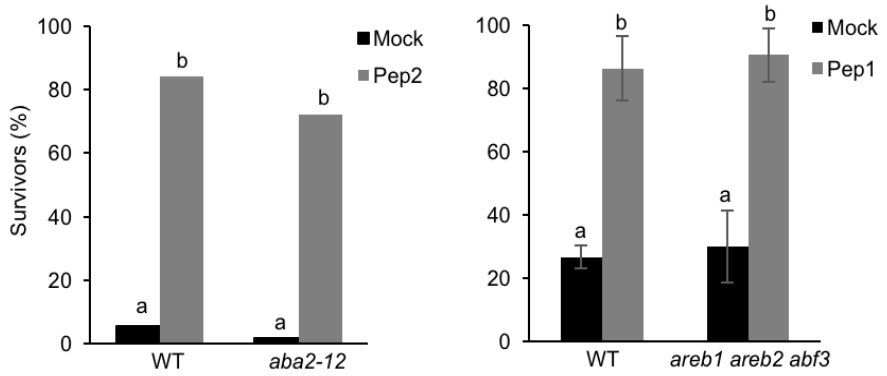

Figure 8: ABA is dispensable for PTST
Survival rate (%) of WT and ABA-related mutant seedlings, with and without 0.1 μg Pep1 or Pep2 pre-treatments, 7 days after exposure to 175 mM NaCl. Data from at least two independent experiments (N >60), error bars indicate standard error. Letters above bars indicate $p < 0.05$ calculated with Tukey's HSD.

Salt damage signaling via PEPR contributes to acquired osmotic tolerance in *A. thaliana*

To assess the functional significance of PTST, I tested the possible involvement and role of PEPR signaling under salt stress, in the absence of exogenous Pep application. To this end, together with the host lab, I determined whether the generation and release of PROPEP-derived peptides occur under sterile salt stress conditions. First, *A. thaliana* expressing PROPEP3-VENUS under the control of the *PROPEP3* regulatory DNA sequences (*pPROPEP3::PROPEP3-VENUS*) was subjected to salt stress. Green fluorescence detected under microscopy indicates the expression of PROPEP3-VENUS in the roots 24 hours after salt exposure (Figure 9A).

To test whether salt-induced PROPEP3 is released under salt stress, immunoblot analyses with PROPEP3-specific antibodies were performed by the host lab on PROPEP3-Venus transgenic plants under salt stress. Immunoblot analysis successfully detected PROPEP3-VENUS of the predicted full-length size (~10.4 + 27 kDa) in the extracellular fraction recovered from the growth media (Figure 9B). This analysis also detected a lower molecular weight PROPEP3-VENUS band, a predominantly induced form following bacterial inoculation (Yamada et al., 2016). These observations indicate that salt-induced damage is capable of releasing PROPEP3 to the extracellular spaces and processing PROPEP3 in a manner similar to that induced upon pathogen challenge. In this respect, a recent study reported that laser-induced physical damage activates PROPEP1 processing into a Pep1-containing short peptide(s) and their release from the tonoplast, although whether this leads to their extracellular release or PEPR binding at the cell surfaces remains to be shown (Hander et al., 2019). These results suggest the existence of complex mechanisms underlying PROPEP processing and release, possibly diverged between PROPEP members.

To test the relevance of PROPEPs/Peps release and the PEPR signaling under salt stress, our collaborators assessed acquisition of osmotic tolerance in seedlings after pre-exposure to mild salt stress. To this end, *pepr1 pepr2* mutant plants and their complement lines overexpressing PEPR1 or PEPR2 (*PEPR1-OE* or *PEPR2-OE*, respectively) were subjected to an acquired osmotic tolerance assay. The chlorophyll contents of seedlings were determined after the osmotic stress as a proxy for acquired osmotic tolerance.

The chlorophyll contents in both *PEPR1-OE* and *PEPR2-OE* plants were significantly higher compared to that of *pepr1 pepr2* plants (Supplementary Figure 1A), indicating a role for PEPRs in acquired osmotic tolerance. In agreement with this, *bak1-5 bkk1-1* plants defective in BAK1-dependent PRR signaling, including that of PEPRs, displayed a significant decrease in acquired osmotic tolerance (Supplementary Figure 1B). In good accordance, I show that PEPR1 and PEPR2 overexpressing plants show enhanced salt tolerance compared

to *pepr1 pepr2* plants when directly exposed to severe salt stress, in the absence of acclimation with exogenous application of MAMPs/DAMPs or pre-exposure to mild salt stress (Figure 9C). Collectively, these data suggest that salt-induced PROPEP3 production and release engage the endogenous PEPR signaling in salt-induced acclimation to osmotic stress.

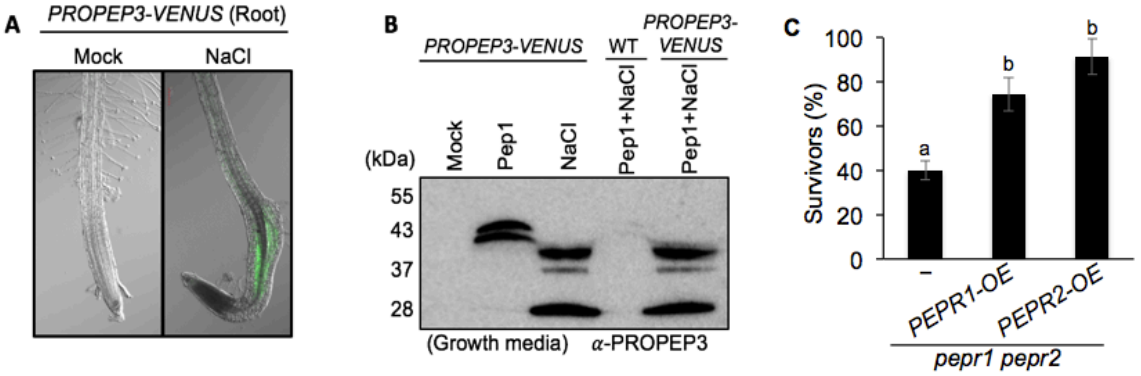

Figure 9: PEPR signaling mediates salt tolerance

A. Microscopy visualization of *A. thaliana* roots expressing PROPEP3-VENUS (*pPROPEP3::PROPEP3-VENUS)* 24 hours after exposure to mock and 150 mM NaCl.

B. Anti-PROPEP3 immunoblot analysis of the growth media where PROPEP3-VENUS seedlings were treated with 0.5 μM Pep1, 150 mM NaCl or the combination of both for 3 days. Representative figure from 2 independent experiments.

C. Survival rate (%) of *pepr1 pepr2* and PEPR-overexpressing seedlings in the *pepr1 pepr2* background, 4 days after exposure to 175 mM NaCl. Data from the average of 3 independent experiments (N >40). Letters above bars indicate p <0.05 calculated using Tukey's HSD.

Pep1 pre-treatment influences the transcriptome dynamics of seedlings under salt stress

To gain mechanistic insight into PTST, transcriptome profiling was performed in WT and *pepr1 pepr2* seedlings with and without Pep1 pre-treatment followed by 0, 3 or 24 hours of salt stress (Figure 10A). These time points were selected in light of a published study that identified the majority of the salt-responsive genes under salt stress for 1 to 24 h (Geng et al., 2013).

To determine the effect of Pep1 application on temporal dynamics of salt-induced transcriptome, transcriptome profiles were obtained at 0, 3 and 24 h after the onset of salt stress, and then compared between mock and Pep1 pre-treated plants. Next, I selected the DEGs during PTST, with the following comparisons: 1) mock vs. Pep1-treated WT plants, and 2) Pep1-treated WT vs. Pep1-treated *pepr1 pepr2* plants for each time point under salt stress. The common DEGs with a cut-off of $|\log_2 (\text{fold change})| \geq 1$ ($p < 0.05$) from these comparisons were used for further analysis. In total, 812 up- and 1163 down-regulated DEGs were obtained from all the three time points tested (Figure 10B). These DEGs were subjected to one minus Pearson correlation complete linkage hierarchical clustering to produce a heat map with 21 clusters (Figure 10C). Among the clusters, clusters 1, 6, 9 and 12, and clusters 7, 8, 10 and 13 were categorized into two main groups of interest based on their expression patterns.

Expression of DEGs in the clusters 1, 6, 9, and 12 is accelerated under salt stress after Pep1 pre-treatment. Functional annotation analysis illuminated significant enrichment of GO terms related to immune responses, and hyperosmotic and salt stress responses. Indeed, several DEGs in these clusters have been reported to influence both defense and salt stress responses. For example, *PEPTIDE TRANSPORTER3* (*AtPTR3*) in the cluster 12 identifies a defense gene that confers salt stress tolerance. *ptr3* mutant plants exhibit poor germination under salt stress and increased susceptibility to *Pst* DC3000, pointing to a critical role for *AtPTR3* in both salt tolerance and bacterial resistance (Karim et al., 2005, 2007).

Clusters 7, 8, 10 and 13 represent DEGs that are salt-inducible but Pep1-repressive. DEGs found in these clusters are mostly involved in salt tolerance including a gene from cluster 7 that encodes a putative Ca^{2+} channel ANNEXIN4 (ANN4) that was recently reported to be regulated by SOS2 and ScaBP8/SOS3 in SOS signaling (Ma et al., 2019). The study shows that the SOS pathway represses the activity of ANN4 to fine-tune salt-induced calcium signal in order to optimize the plants' responses to prolonged salt stress. In addition to that, the loss of *HAI3,* from cluster 13, results in increased proline and osmoregulatory solutes

production that leads to enhance dehydration tolerance (Bhaskara et al., 2012). Thus, Pep1 repression of *ANN4, HAI3* and related clusters of DEGs could promote salt tolerance.

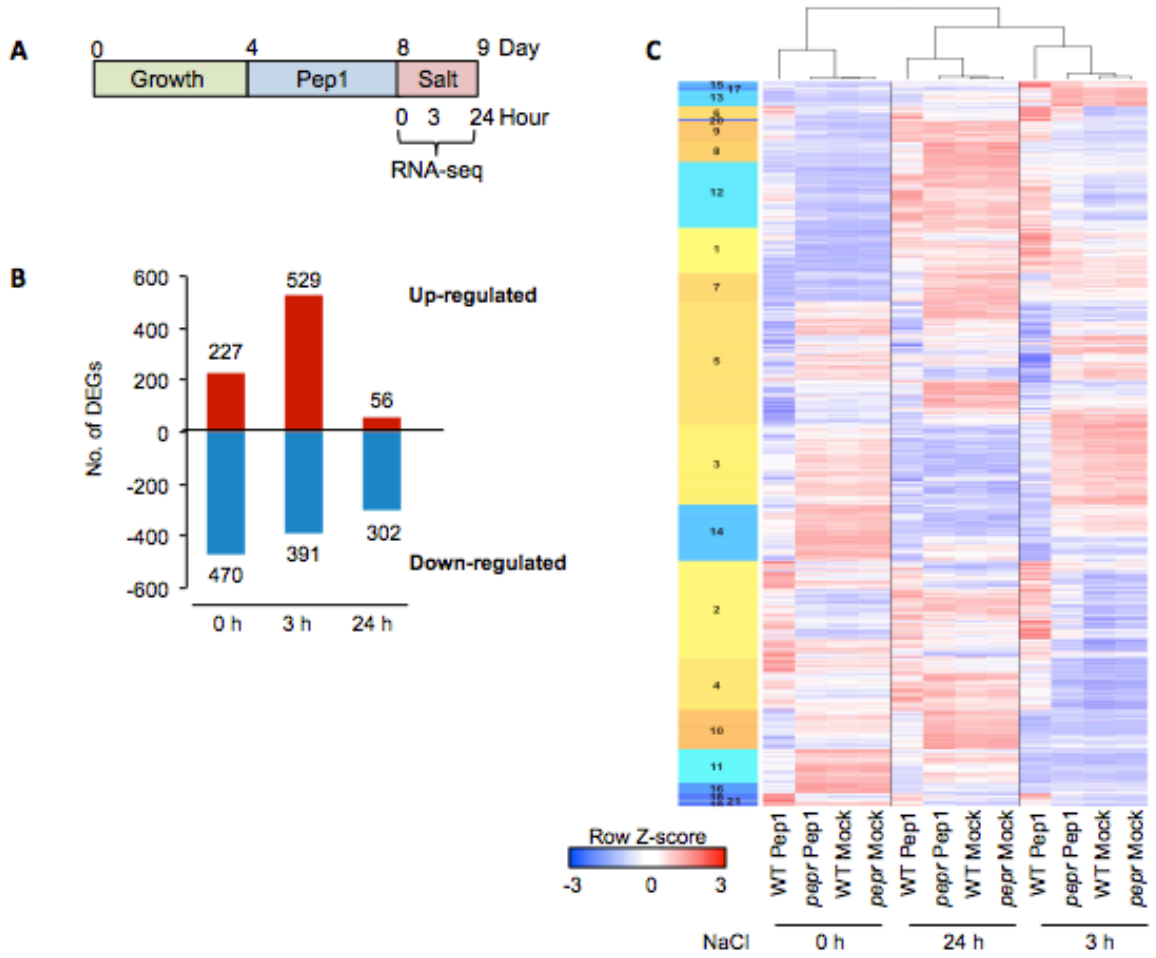

Figure 10: Pep1 pre-treatment influences the transcriptome dynamics of seedlings under salt stress

A. Treatment scheme for WT and *pepr1 pepr2* seedlings used for transcriptome profiling.

B,C. Graph (B) and heat map (C) of up- and down-regulated PTST DEGs after 0 h, 3 h and 24 h of exposure to 175 mM NaCl. Clustering performed according to one minus Pearson correlation complete linkage hierarchical clustering ($|\log_2(\text{fold change})| \geq 1$).

WRKY18/WRKY40 transcription factors contribute to PTST, in part, by suppressing EDS1 function

Genes with similar expression profiles tend to carry similar *cis* regulatory elements in their promoter regions (Rombauts et al., 2003). Thus, with the information from transcriptome profiling, I sought to identify potential PTST regulator(s) by mining common *cis* regulatory elements in the -1000 bp regions upstream of the transcriptional start sites on only the sense strand of PTST DEGs. This was performed with a motif enrichment analysis tool, CentriMo (Bailey and Machanick, 2012). The algorithm identified 38 significantly enriched (*E*-value < 0.00001) transcription factor binding sites, 24 of which belong to the WRKY family, indicating an over-representation (Table 2). This prompted me to test the possibility that WRKY transcription factors are involved in the regulation of PTST.

Among the 74 WRKY transcription factors in *A. thaliana*, I put an initial focus on WRKY18, WRKY40 and WRKY33 on the basis of their elaborate roles in PTI signaling (Birkenbihl et al., 2016). In addition to the three WRKY transcription factors, WRKY60 was also included as a potential candidate due to high sequence and structural similarities with WRKY18 and WRKY40 (Xu et al., 2006). Due to the complex interactions and cross-regulations among WRKY18, WRKY40 and WRKY60 (Xu et al., 2006; Yan et al., 2013), single, double and triple mutant plants were tested for PTST. Of the mutants tested, *wrky18 wrky40* double mutant plants failed to confer PTST while all other mutant combinations showed the WT-like phenotype (Figure 11). These observations indicate that WRKY18 and WRKY40 both contribute to PTST. Henceforth, *wrky18 wrky40* double mutant plants were selected for subsequent analyses.

A second *wrky18 wrky40* mutant allele is also impaired in PTST, confirming the earlier conclusion (Figure 12A). The inability of *wrky18 wrky40* plants to confer PTST demonstrated a role for WRKY18/WRKY40 as positive regulators in PTST. To authenticate their role in transcriptional regulation of PTST, the expression a direct target, *PTR3* (Birkenbihl et al., 2017), from the cluster 12 as previously described, was analyzed. The expression of *PTR3* was induced under salt stress and PTI, and also synergistically induced under PTST (Figure 12B). However, *PTR3* induction levels were reduced in *wrky18 wrky40* plants during PTST. Thus, WRKY18/WRKY40 positively contribute to PTST.

Table 2: *In silico* analysis on PTST DEGs for transcription factor binding sites significantly enriched (*E*-value < 0.00001) on the -1000 bp upstream of transcriptional start site. Analysis performed with CentriMo (http:// meme-suite.org/tools/centrimo).

Transcription factor	Motif ID	Binding site consensus	E-value	p-value	Bin width
ANAC047	NAC_tnt.ANAC047_colamp_a_d1	CACGT	3.00E-20	7.00E-29	130
ATAF1	NAC_tnt.ATAF1_colamp_a_d1	ACGTR	2.30E-13	5.30E-22	134
WRKY40	WRKY_tnt.WRKY40_colamp_a_m1	NDAAAAGTCAAMR	6.90E-13	1.60E-21	160
WRKY43	WRKY_tnt.WRKY43_colamp_a_m1	WDAAAAAGTCAACGN	1.60E-11	3.70E-20	152
WRKY29	WRKY_tnt.WRKY29_colamp_a_m1	MAAAGTCAACKNH	2.50E-11	5.90E-20	155
WRKY14	WRKY_tnt.WRKY14_colamp_a_m1	AAAAGTCAACGNH	2.60E-11	6.20E-20	144
WRKY65	WRKY_tnt.WRKY65_col_a_m1	AAAAGTCAACG	9.80E-11	2.30E-19	160
WRKY33	WRKY_tnt.WRKY33_col_a_m1	AAAAGTCAACG	1.20E-10	2.80E-19	148
WRKY3	WRKY_tnt.WRKY3_col_a_m1	AAAAGTCAACG	1.50E-10	3.40E-19	162
WRKY18	WRKY_tnt.WRKY18_col_a_m1	VAARGTCAASR	2.50E-10	5.80E-19	161
WRKY22	WRKY_tnt.WRKY22_col_m1	AAAAGTCAACKNH	4.50E-10	1.10E-18	152
WRKY27	WRKY_tnt.WRKY27_colamp_a_m1	AAAAGTCAACKNY	4.80E-10	1.10E-18	160
bZIP68	bZIP_tnt.bZIP68_col_a_m1	TGCCACGTSABCWHH	4.90E-10	1.20E-18	99
bHLH157	bHLH_tnt.bHLH157_col_a_m1	HMAAWTHNDWCACGTCWCYK	5.00E-10	1.20E-18	135
AT3G42860	zfGRF_tnt.AT3G42860_col_a_m1	HAAAGTCAACG	8.10E-10	1.90E-18	150
WRKY25	WRKY_tnt.WRKY25_col_a_m1	AAWAGTCAACG	1.30E-09	3.10E-18	148
WRKY30	WRKY_tnt.WRKY30_col_a_m1	AAAGTCAACGN	1.40E-09	3.40E-18	142
WRKY15	WRKY_tnt.WRKY15_col_b_m1	AAAAGTCAACG	1.90E-09	4.50E-18	155
BAM8	BES1_tnt.BAM8_col_a_m1	YCACACGTGYSAANT	7.80E-09	1.80E-17	131
WRKY71	WRKY_tnt.WRKY71_col_a_m1	AAAAGTCAACG	8.20E-09	1.90E-17	161
WRKY21	WRKY_tnt.WRKY21_col_m1	AAAAGTCAACG	9.10E-09	2.10E-17	150
BIM2	bHLH_tnt.BIM2_col_v3b_m1	CACGTGMCHHNCACG	9.10E-09	2.10E-17	105
WRKY31	WRKY_tnt.WRKY31_col_a_m1	DDNNHWRHHAAAGTCAACG	1.10E-08	2.70E-17	158
AT1G78700	BZR_tnt.At1g78700_colamp_a_m1	BYRCACGTGTGNATT	1.80E-08	4.10E-17	137
BIM1	bHLH_tnt.BIM1_colamp_a_m1	HVTCACGTGACHHHYAYVTNNN	3.80E-08	9.10E-17	100
WRKY42	WRKY_tnt.WRKY42_colamp_a_m1	HWDNHWWRGTCAACGNHDDK	4.90E-08	1.20E-16	154
PIF7	bHLH_tnt.PIF7_col_a_m1	SDKRDWGCCACGTGG	6.90E-08	1.60E-16	98
GT3a	Trihelix_tnt.GT3a_col_a_m1	RRCACGTGTHWAAWDTD	9.30E-08	2.20E-16	160
WRKY17	WRKY_tnt.WRKY17_colamp_a_m1	WAAAAGTCAACGN	1.10E-07	2.60E-16	151
AT4G18890	BZR_tnt.At4g18890_colamp_a_m1	YGCACGTGTGR	1.50E-07	3.40E-16	138
WRKY8	WRKY_tnt.WRKY8_col_m1	NAAAAAGTCAACGNH	1.70E-07	4.10E-16	155
WRKY46	WRKY_tnt.WRKY46_colamp_a_m1	MAAAGTCAACG	2.40E-07	5.60E-16	162
WRKY59	WRKY_tnt.WRKY59_col_a_m1	HAAAAGTCAAMN	3.80E-07	8.90E-16	162
WRKY55	WRKY_tnt.WRKY55_col_a_m1	DNCGTTGACTTT	4.30E-07	1.00E-15	157
bHLH34	bHLH_tnt.bHLH34_col_m1	GTGNNNRVCACGTGBCDNHDBDH	9.90E-07	2.40E-15	130
WRKY26	WRKY_tnt.WRKY26_col_a_m1	AAAAGTCAACGNY	2.50E-06	5.80E-15	163
bHLH104	bHLH_tnt.bHLH104_col_b_m1	GVCACGTGBCDDCMNSKGSM	4.30E-06	1.00E-14	109
WRKY6	WRKY_tnt.WRKY6_col_a_m1	CGTTGACTWWDDYWDWNHH	4.40E-06	1.00E-14	153

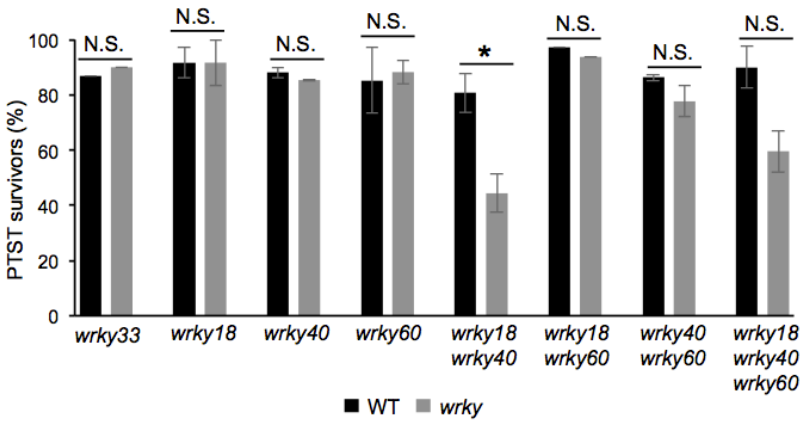

Figure 11: WRKY18/WRKY40 contributes to PTST
Survival rate (%) of WT and *wrky* mutant seedlings, 7 days after exposure to 175 mM NaCl following 0.1 μM Pep1 pre-treatment. N >30, error bars indicate standard error. *p <0.05 calculated using Tukey's HSD, N.S.- Not significant.

In the effort to dissect the regulatory control of PTST by WRKY18 and WRKY40, I referred to a previous study on the flg22-inducible direct binding targets of WRKY18 and WRKY40 (Birkenbihl et al., 2016). Among the binding targets was *EDS1* that has been shown to attenuate acquired osmotic tolerance (Ariga et al., 2017). Evidence also shows that *EDS1* expression is repressed under salt stress (Prasad et al., 2016). These studies point to the importance of *EDS1* suppression as a critical step in conferring salt/osmotic tolerance. Previous studies have also reported WRKY18 and WRKY40 as suppressors of EDS1 in PTI and disease resistance (Birkenbihl et al., 2016; Pandey et al., 2010; Schön et al., 2013).

Thus, to investigate the relationship between WRKY18/WRKY40 and EDS1 in PTST, *eds1, wrky18 wrky40* and *wrky18 wrky40 eds1* mutant plants were subjected to the PTST assay. WT-like PTST phenotype was observed in *eds1* single mutant plants whereas PTST was attenuated in *wrky18 wrky40* plants (Figure 12A). However, the loss of EDS1 in the *wrky18 wrky40* background restored PTST to WT-like levels (Figure 12A). This suggests that WRKY18/WRKY40 is involved in the suppression of EDS1 function during PTST.

To validate this, I next examined expression of *EDS1* during PTST in WT and *wrky18 wrky40* plants. Expression of *EDS1* is retained at basal levels in WT seedlings but up-regulated in *wrky18 wrky40* seedlings during PTST (Figure 12C). In light of the previously described role for WRKY18/WRKY40 as transcriptional repressors (Pandey et al., 2010; Schön et al., 2013), these observations indicate that *EDS1* de-repression compromises PTST in *wrky18 wrky40* plants.

I next assessed the possible dynamics of WRKY18 and WRKY40 expression during PTST with immunoblot analyses. Plants expressing a functional HA-tagged WRKY18 or WRKY40 protein driven by their own promoters in the corresponding loss-of-function mutant backgrounds (*pWRKY18::WRKY18-HA/wrky18* and *pWRKY40::WRKY40-HA/wrky40*, respectively) were subjected to PTST. Immunoblot analyses with anti-HA antibodies revealed that Pep1 pre-treatment promoted the accumulation of both WRKY18 and WRKY40 specifically during an early phase under salt stress (Figure 13A). Although WRKY18 protein were detected in the non-induced state, its abundance was clearly increased with Pep1 pre-treatment. Accumulation of WRKY18 in the non-induced state was due to high-level basal protein accumulation in the transgenic line used (Birkenbihl et al., 2016).

Interestingly, the mRNA expression patterns of *WRKY18* and *WRKY40* were not followed by their respective protein expression patterns (Figure 13B). *WRKY18* mRNA levels were not elevated by Pep1 pre-treatment under salt stress at least for 0 to 24 h, while in contrast WRKY18 protein levels clearly increased with Pep1 pre-treatment (Figure 13A). On the other hand, the expression of *WRKY40* was rather reduced with Pep1 pre-treatment in

marked contrast to the increased protein levels (Figure 13B). This suggests a role for post-transcriptional regulation in the accumulation of WRKY18 and WRKY40 during PTST.

I thus assessed whether Pep1 pre-treatment stabilizes WRKY18 and WRKY40 during salt stress. To this end, I treated mock and Pep1-treated WRKY18-HA and WRKY40-HA seedlings with a 26S proteasome inhibitor, MG132, prior to salt stress. As previously observed, WRKY18 and WRKY40 abundance decreased under salt stress but MG132 treatment allowed stable accumulation of WRKY18 and WRKY40, of which the extent was comparable to that of Pep1 pre-treatment (Figure 13C).

Besides WRKY18/WRKY40, the CAMTA3 transcription factor binds and represses the expression of *EDS1* in response to pathogen challenge (Du et al., 2009) and negatively regulates salt tolerance (Prasad et al., 2016). Thus, I tested whether CAMTA3 contributes to PTST as well. Pre-treatment with flg22 successfully induced salt tolerance in *camta3-D*, a loss-of-function CAMTA3 mutant that is impaired in PTI and ETI (Figure 14), indicating that the function of CAMTA3 is not required for PTST.

Thus far, the evidence obtained supports the hypothesis that Pep1 pre-treatment promotes WRKY18 and WRKY40 accumulation by protecting the proteins from proteasomal degradation under salt stress. WRKY18/WRKY40 then serve to attenuate EDS1 function, at least at the transcriptional level, to confer PTST.

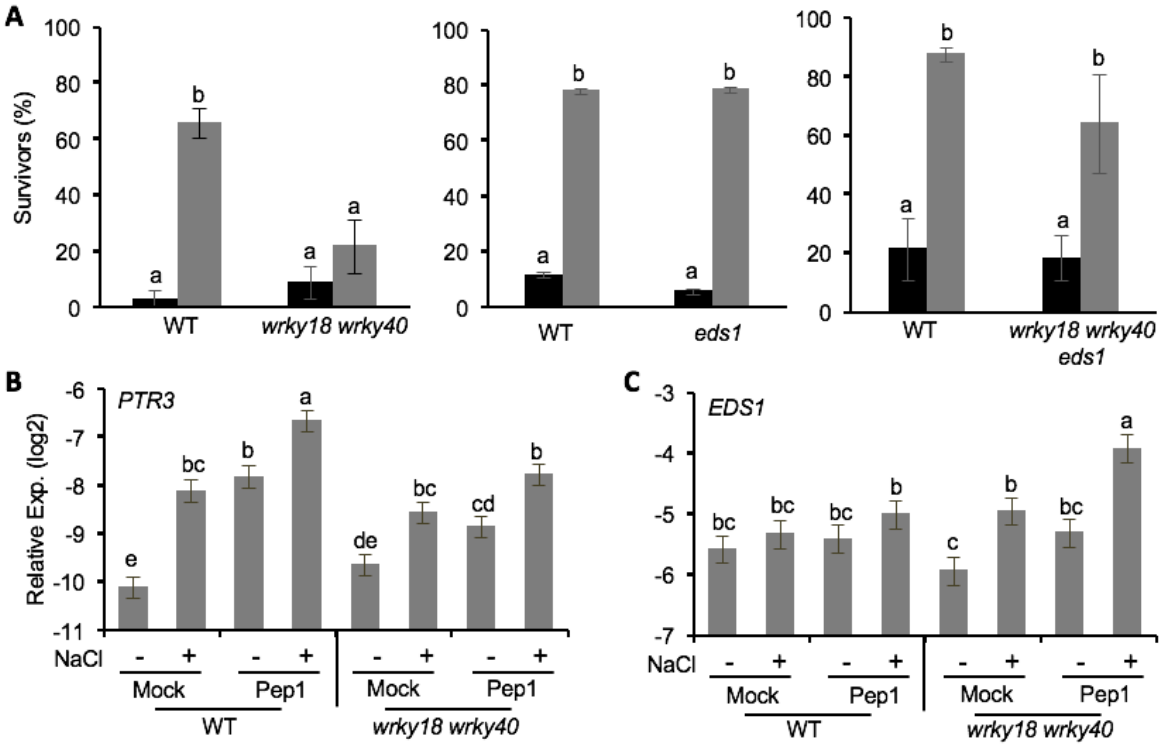

Figure 12: WRKY18/WRKY40 regulate PTST in part by suppressing *EDS1*

A. Survival rate (%) of WT and *wrky18 wrky40 eds1* double and triple mutants, with (black) and without (gray) 0.1 μM Pep1 pre-treatment, 9 days after exposure to 175 mM NaCl. Data from at least two independent experiments (N >60), error bars indicate standard error. Letters above bars indicate p <0.05 calculated using Tukey's HSD.

B,C. qRT-PCR analysis of *PTR3* and *EDS1* expressions in 9-day-old WT and *wrky18 wrky40* seedlings, with and without 0.1 μM Pep1 pre-treatment, 3 hours after exposure to 175 mM NaCl. Normalized expressions (against *Actin2* values) from 3 independent experiments with 3 biological replicates each. Error bars indicate standard error. Letters above bars indicate p <0.01 calculated using linear model.

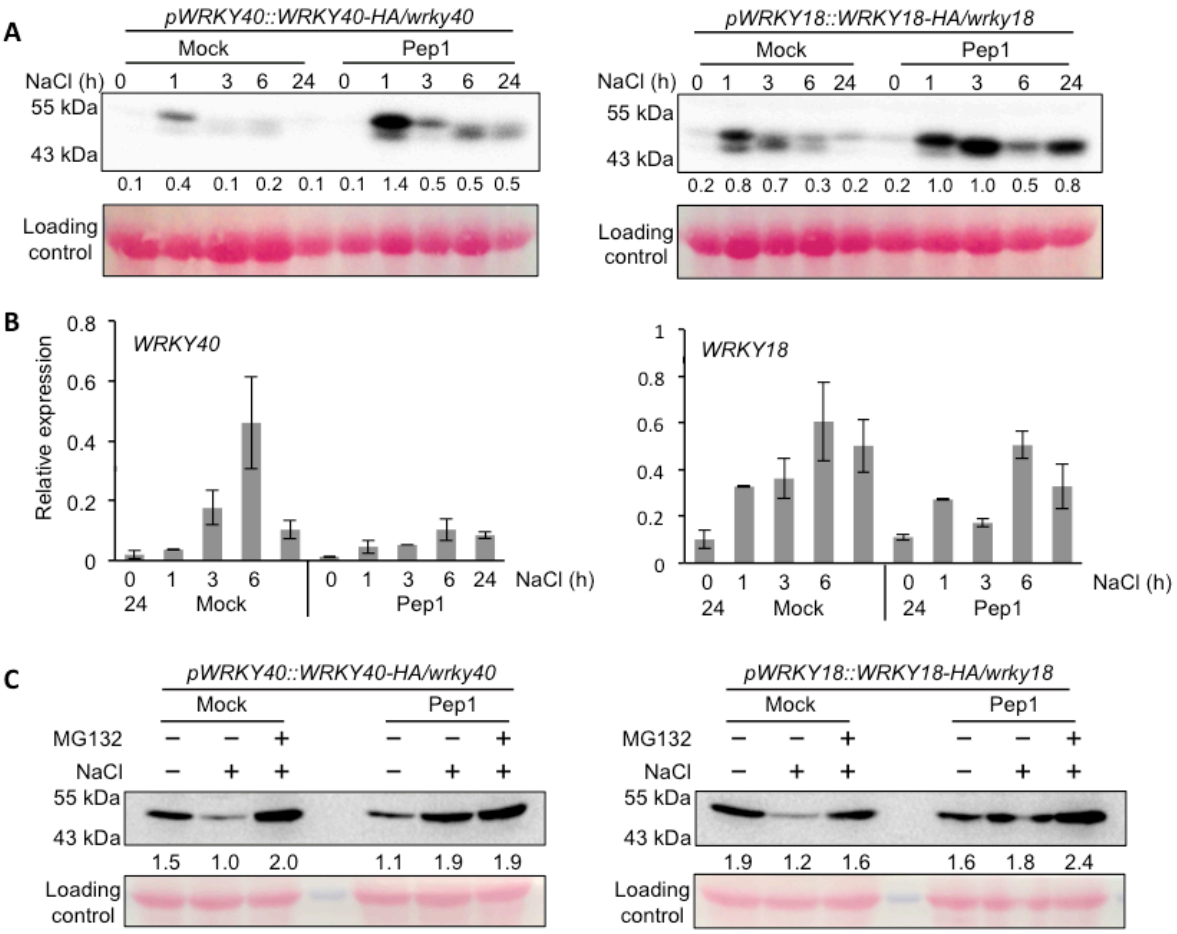

Figure 13: Pep1 pre-treatment stabilizes WRKY18 and WRKY40 under salt stress

A. Anti-HA immunoblot analysis of 9/10-day-old WRKY40-HA and WRKY18-HA seedlings after the indicated period of exposure to 175 mM NaCl, with or without 0.1 μM Pep1 pre-treatment. A representative figure is shown from 3 independent experiments. Numbers in between blots indicate band intensities relative to loading control.

B. qRT-PCR analysis of *WRKY40* and *WRKY18* expressions in 9/10-day-old WT seedlings, after indicated period of exposure to 175 mM NaCl, with or without 0.1 μM Pep1 pre-treatment. Expression levels were normalized against *Actin2* expression values. Representative figure from 3 independent experiments with 3 biological replicates each. Error bars indicate standard errors.

C. Anti-HA immunoblot analysis of mock or Pep1 pre-treated 9-day-old WRKY40-HA and WRKY18-HA seedlings with or without 0.05 μM MG132 treatment, after 3 hours of exposure to 175 mM NaCl. A representative figure from 3 independent experiments is shown. Numbers in between blots indicate band intensities relative to loading control.

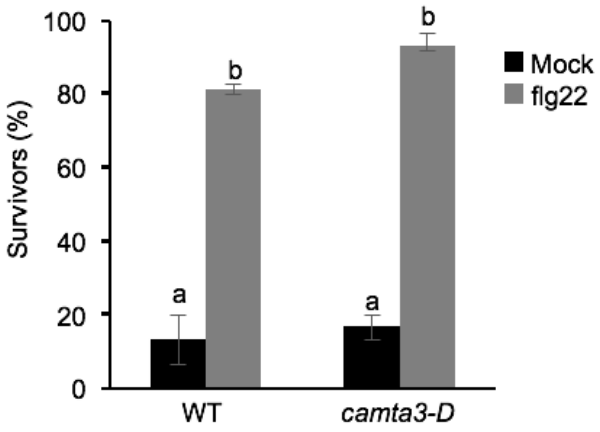

Figure 14: CAMTA3 transcription factor does not contribute to PTST
Survival rate (%) of WT and CAMTA3 dominant negative mutant, with and without 0.1 μM flg22 pre-treatment, 7 days after exposure to 175 mM NaCl. Data from at least two independent experiments (N >60), error bars indicate standard error. Letters above bars indicate $p < 0.05$ calculated using Tukey's HSD.

Non-pathogenic bacteria confer PTST

To assess the biological relevance of my findings in a broader and more native context, I tested whether PRR recognition of microbes confers PTST, as shown above for that of MAMPs. To this end, seedlings were spray-inoculated with different strains of *Pst* DC3000 prior to salt stress. Relative to MAMP/DAMP-triggered salt tolerance, I also compared the effects of ETI signaling activation on salt tolerance. *Pst* DC3000 *ΔhrpS* that is defective in effector delivery was used as a PTI inducer, whereas *Pst* DC3000 *AvrRpm1* and *Pst* DC3000 *AvrRps4* were used as NDR1- and EDS1-mediated ETI inducers, respectively.

Interestingly but not unexpectedly, pre-inoculation with *Pst* DC3000 *ΔhrpS* significantly enhanced seedlings survival under salt stress, while in contrast *Pst* DC3000 *AvrRpm1* and *Pst* DC3000 *AvrRps4* did not (Figure 15A). This indicates that non-pathogenic PTI-inducing bacteria are more potent at conferring salt tolerance compared to ETI-inducing bacteria. Henceforth, *Pst* DC3000 *ΔhrpS* is used as a bacterial elicitor in subsequent assays.

Bacterium-triggered salt tolerance was compromised in PTI-impaired *bak1-5 bkk1-1* and *fls2 efr* plants (Figure 15B-C), as also seen in MAMPs/DAMPs-triggered salt tolerance (Figure 4B, 5A). The failure of *Pst* DC3000 *ΔhrpS* to trigger salt tolerance in these mutant plants point to its similar genetic requirements to that of MAMPs/DAMPs-triggered salt tolerance. Further validation with *wrky18 wrky40* plants showed compromised bacterium-triggered salt tolerance as also observed with Pep1 pre-treatment (Figure 12A, Figure 15D). These observations indicate that bacterium-triggered salt tolerance relies on common genetic components to that of MAMPs/DAMPs-triggered salt tolerance.

To authenticate bacterium-triggered salt tolerance, inoculation effects of another non-pathogenic bacterium, *Pseudomonas fluorescence* (*Pfo*) was tested. Consistent with Pep1- and *Pst* DC3000 *ΔhrpS*-triggered salt tolerance, *Pfo* successfully conferred salt tolerance in a manner dependent on PTI signaling components (Figure 16A). I next tested whether live bacteria, e.g. through delivery of proteins or metabolites to the host, contributed to bacterium-triggered salt tolerance. To this end, *Pfo* and *Pst* DC3000 *ΔhrpS* were heat-killed and then applied to seedlings. Remarkably, pre-treatments with both heat-killed bacterial strains successfully conferred PTST in a manner dependent on PTI signaling components (Figure 16B-C). This demonstrates that *A. thaliana* seedlings do not require viable bacteria in acquiring salt stress tolerance, making it most likely that recognition of their MAMPs is sufficient to induce salt tolerance in the host plant. To our best knowledge, this study for the first time provides compelling evidence that PRR recognition of bacteria (most likely through that of MAMPs) promotes plant adaptation to salt stress.

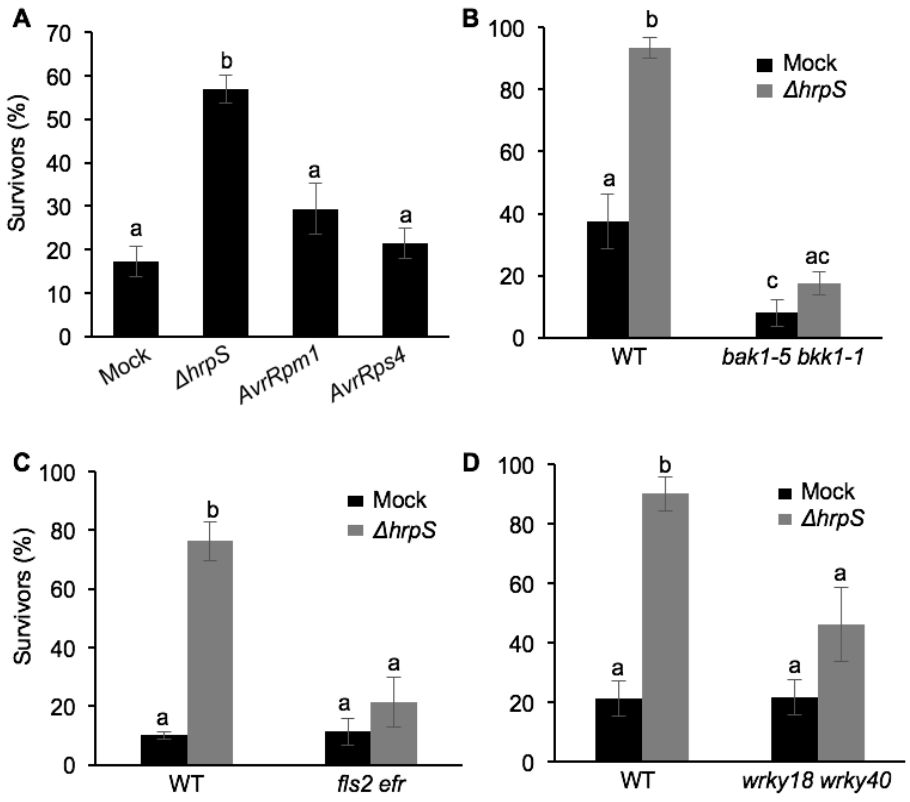

Figure 15: Non-pathogenic bacteria confer salt tolerance via PTST

A. Survival rate (%) of WT seedlings with and without PTI- or ETI-inducing *Pst* DC3000 bacterial strain inoculation, 5 days after exposure to 175 mM NaCl. Data from 3 independent experiments (N >60), error bars indicate standard error. Letters above bars indicate p <0.05 calculated using Tukey's HSD.

B-D. Survival rate (%) of WT, (B, C) PTI mutants and (D) *wrky18 wrky40* seedlings with and without *Pst* DC3000 *ΔhrpS* spray-inoculation, 5 days (B, C) and 6 days (D) after exposure to 175 mM NaCl. Data from 3 independent experiments (N >60), error bars indicate standard error. Letters above bars indicate p <0.05 calculated using Tukey's HSD.

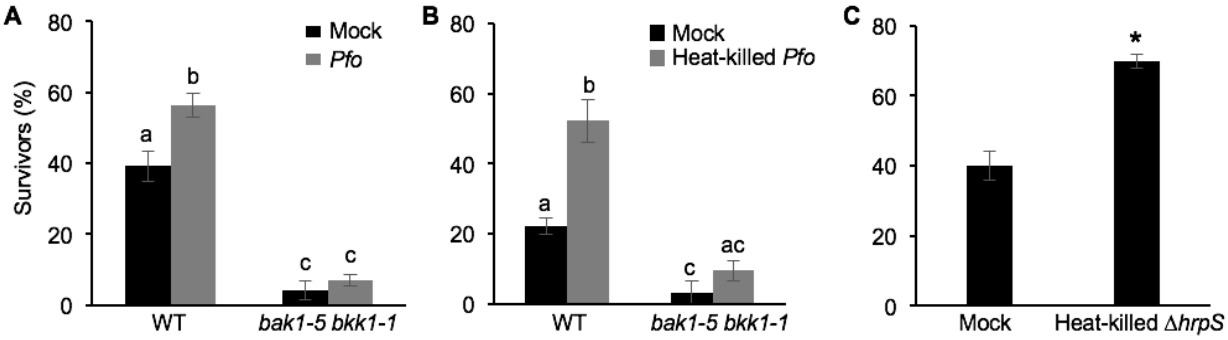

Figure 16: Viable and heat-killed non-pathogenic bacteria confer PTST

A. Survival rate (%) of WT and *bak1-5 bkk1-1* seedlings, with and without *Pfo* spray-inoculation, 5 days after exposure to175 mM NaCl. Data from 3 independent experiments (N >60), error bars indicate standard error. Letters above bars indicate $p < 0.05$ calculated using Tukey's HSD.

B. Survival rate (%) of WT and *bak1-5 bkk1-1* seedlings, with and without heat-killed *Pfo* pre-treatment, 4 days after exposure to 175 mM NaCl. Data from the average of 3 independent experiments (N >60). Letters above bars indicate $p < 0.05$ calculated using Tukey's HSD.

C. Survival rate (%) of WT seedlings, with and without heat-killed *Pst* DC3000 *ΔhrpS* pre-treatment, 4 days after exposure to 175 mM NaCl. Data from the average of 3 independent experiments (N >60). *$p < 0.05$ calculated using two-tailed t-test.

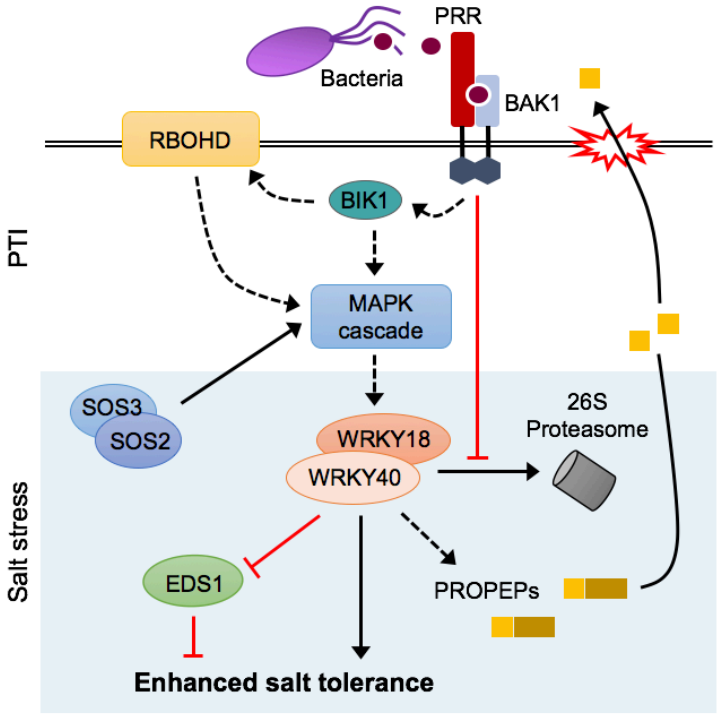

Figure 17: Pattern-triggered salt tolerance working model
Under salt stress, MAMPs/DAMPs recognition by PRRs activates PTI signaling, leading to WRKY18/WRKY40 stabilization and accumulation. WRKY18/WRKY40 suppress EDS1 function to confer salt tolerance, resulting in PTST. Salt damage also induces PROPEPs processing and release to the extracellular for PEPR recognition, creating a positive feedback loop to induce PTST. In parallel, SOS2 and SOS3 converge into PTI signaling to engage in PTST signaling via a mechanism that remains unknown. Solid lines indicate pathways revealed in this study. Dotted lines indicate pathways described in published literature.

DISCUSSION

Here, I report a positive relationship between plant responses to biotic stress and salt stress, in which PRR-mediated defense signaling activation leads to enhanced salt tolerance in *A. thaliana*, in a phenomenon designated PTST. Immunogenic pattern recognition by cognate PRRs induces PTI signaling, which involves WRKY18/WRKY40 transcription factors to attenuate EDS1 function. This seems to provide a means to avoid over-activation of costly defenses and also to confer salt tolerance (Figure 17). This study also provides the first evidence for crosstalk between PRR and SOS signaling during PTST. I concluded this study with that non-pathogenic bacteria are also capable of inducing salt tolerance, pointing to the biological relevance of PTST.

I laid the groundwork in this study by showing that recognition of a wide range of molecular patterns, e.g. MAMPs (flg22 and elf18) and DAMPs (Pep1-Pep4), by their cognate PRRs leads to enhanced salt tolerance in *A. thaliana* seedlings (Figure 4, Table 1). This rectifies previous studies that reported the contribution of individual PRRs and MAMPs or DAMPs in salt tolerance (Brotman et al., 2012; Espinoza et al., 2017; Feng et al., 2018; Nakaminami et al., 2018; Zhao et al., 2018).

Of note, in spite of the previously reported role for chitin (perceived via CERK1) in salt tolerance (Brotman et al., 2012; Espinoza et al., 2017), chitin pre-treatment failed to confer PTST under my conditions (Figure 5). The inability of chitin to confer PTST may be due to differences in the requirements for downstream signaling components in chitin-induced PTI signaling, such as the dispensability for BAK1 and the restricted role of the RLCK PBL27 (Couton and Zipfel, 2016). In any possible scenario, it seems likely that different PRRs not uniformly but in part differentially mediate salt tolerance in a context-dependent manner. Nevertheless, my findings indicate that early steps downstream of PRRs are shared between PTI and PTST signaling pathways, and that the balance between PTI and PTST activation is determined according to the extent of salt stress.

In addition to cognate receptors, I have determined the genetic requirements and dissected the signaling pathway(s) downstream of PRRs in PTST. I show that authentic receptor complexes and PTI signaling components are required to mount PTST (Figure 6). Collectively, these data indicate that PTST and PTI share signaling components, and suggest that PTST utilizes (an early part of) the PTI signaling pathway.

sos mutants failed to confer PTST whilst retaining early PTI signaling (Figure 7A-C). *sos2* and *sos3* plants are incapable of sustaining MAMP-induced MAPK activation, and these mutants show reduced MAPK activation following salt exposure (Figure 7D). This suggests a requirement for SOS2/SOS3 in late PTI activation, indicating a convergence between PTI and SOS signaling in PTST. Future work to study the interactions between SOS signaling and PTI signaling components will facilitate better understanding on signal integration between the two pathways.

In this study, I present mechanistic insight into PTST in which salt inflicts cellular damage that leads to the expression, processing and release of full-length PROPEPs and shorter, possibly mature forms containing Peps, to activate PEPR signaling toward PTST (Figure 18). This scheme is supported by the successful detection of PROPEP3-VENUS in the extracellular following salt stress (Figure 9A-B). In principle, the released peptides will be recognized by PEPRs leading to PTI activation to enable acquisition of salt/osmotic tolerance. This is supported by the requirement for PEPRs in mounting acquired osmotic and salt tolerance (Figure 9C-D). Under salt stress, a lower survivor ratio is also evident in mock-treated *bik1 pbl1* and *bak1-5 bkk1-1* plants compared to WT plants, possibly due to the failure to engage the endogenous PEPR-mediated PTI signaling activation to confer PTST (Figure 6C, Figure 15B, Figure 16A-B).

A recent study reported that physical damage could trigger PROPEP processing into short, possibly mature forms of Pep1 (Hander et al., 2019). This is also reflected in the present study where smaller PROPEP3-derived peptides were detected in the extracellular spaces (Figure 9C). Interestingly, PROPEP3-derived fragments of smaller sizes was also detected during or after bacterial infection (Yamada et al., 2016). This suggests the possibility that PROPEP3 undergoes similar processing during salt stress and bacterial infection, hinting at an overlapping mechanism in bacterial perception and salt stress sensing. However, the identity of the smaller peptides remains to be determined.

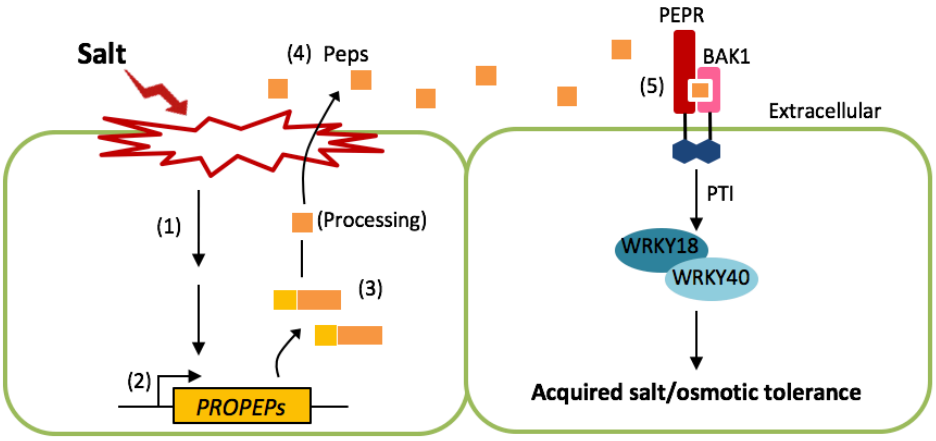

Figure 18: PEPR-mediated acquisition of salt/osmotic tolerance
Salt-inflicted damage on plant cells induces the expression of *PROPEPs* for the production of PROPEPs and processed Peps peptides. Peps are released to the extracellular through the damage site and are recognized by PEPRs of neighboring cells. This leads to PTI activation and subsequently, WRKY18/WRKY40-dependent acquisition of salt/osmotic tolerance.

A combination of transcriptome profiling, *in silico* data mining and genetic analyses indicate WRKY18/WRKY40 transcription factors as positive regulators of PTST (Figure 11, Figure 12). Cross-referencing the transcriptome profiles obtained from this study with published resources (Birkenbihl et al., 2016) show that 51.8% of PTST target genes are also WRKY18/WRKY40 target genes in PTI, as indicated by their altered expression in *wrky18 wrky40* mutant plants after flg22 application for 2 h. The presence of non-WRKY18/WRKY40 targets indicates the existence of an alternative pathway(s) regulating PTST. The influence of these pathways on each other and their integration during PTI and PTST require further study.

I have obtained an inventory of the transcriptional targets for WRKY18/WRKY40 in PTST. Previous studies drove my attention to the key basal defense regulator, EDS1. It was previously reported that the activation of EDS1-mediated immunity negatively affects acquisition of osmotic tolerance after mild salt stress (Ariga et al., 2017; Figure 9). By contrast, my study shows that defense activation through PRRs positively influences salt/osmotic stress tolerance. Apparent discrepancy between these studies can be reconciled with the evidence that PRR signaling leads to salt tolerance through WRKY18/WRKY40-mediated attenuation of EDS1 function (Figure 12A). This seem to take place at least at the mRNA level since *EDS1* is de-repressed in *wrky18 wrky40* mutant plant during PTST (Figure 12C). As such, in the event that EDS1 function is repressed due to genetic disruption (as in *eds1*) or WRKY18/WRKY40-mediated suppression (as in WT), plants are capable of PTST. In contrast, when EDS1 expression is de-repressed in the absence of WRKY18/WRKY40- PTST is compromised (Figure 12, Figure 19).

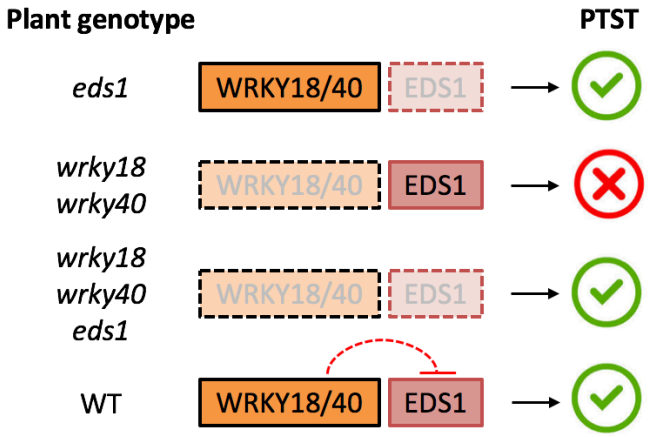

Figure 19: WRKY18/WRKY40 attenuation of EDS1 function is key in PTST
Loss of WRKY18/WRKY40 allows high activation of EDS1, thereby penalizing salt tolerance, whereas loss of EDS1 leads to PTST even in the absence of WRKY18/WRKY40. Thus, a major role of WRKY18/WRKY40 in PTST is attenuation of EDS1.

I further unveiled that Pep1 pre-treatment stabilizes WRKY18 and WRKY40 proteins, which otherwise undergo 26S proteasome-mediated degradation under salt stress (Figure 13). Thus, PRR signaling modulates the abundance of WRKY18/WRKY40 proteins via inhibition of the 26S proteasome degradation, which consequently affects the expression level of *EDS1* under salt stress. This gains insight into the mechanisms behind WRKY18/WRKY40 attenuation of EDSI function following MAMP/DAMP recognition.

I reason that WRKY18/WRKY40 attenuation of EDS1 function during PTST represents a resource-conservation strategy under salt stress. Defense activation is costly and causes diversion of limited resources away from other biological processes including salt/osmotic stress tolerance (Bolton, 2009; Huot et al., 2014). In this aspect, WRKY18/WRKY40 may function as a molecular switch downstream of PRRs to positively regulate PTST by negatively regulating strong defense activation (Figure 11; Birkenbihl et al., 2016).

Plants also developed a coping mechanism to fine-tune their defense outputs for fitness by aborting the execution of costly NLR-triggered ETI (Hatsugai et al., 2017). Hence, tight regulations on NLRs serve to prevent autoimmunity that comes with the expense of other biological processes. For instance, the NLR ACQOS confers biotic resistance in *A. thaliana* via EDS1-mediated ETI. Exposure to osmotic stress triggers ACQOS mis-regulation, which leads to the activation of EDS1-mediated autoimmunity and consequently lowers the

ability to acquire osmotic tolerance (Ariga et al., 2017).

Such control of ETI for abiotic stress tolerance is pronounced in other abiotic stresses and by different NLRs as well. The NLR CHS3 causes EDS1-dependent autoimmunity under cold stress, at the cost of plant growth and cold stress tolerance. Accordingly, *chs3-1* mutant plants show enhanced cold tolerance (Yang et al., 2010). Indeed, I provide evidence that weakly virulent bacteria, *Pfo* and *Pst* DC3000 *ΔhrpS*, which induce low-level defense activation could confer PTST, while in contrast, avirulent bacteria *Pst* DC3000 *AvrRps4* that triggers strong defense activation via EDS i.e. ETI failed to confer PTST (Figure 15). It is thus conceivable that activation of EDS1-mediated defense penalizes abiotic stress tolerance.

Of note, ETI triggered upon recognition of *Pst* DC3000 *AvrRpm1* does not require EDS1 but still compromises salt tolerance. In a similar report, a constitutively active allele of the CC-NLR ADR1, which triggers ETI via NDR1 (and not EDS1), also compromises salt and heat tolerance (Chini et al., 2004). This could be attributable to the recruitment of EDS1 in NDR1-mediated ETI (Bhandari et al., 2019). Noteworthy, ADR1 also confers drought tolerance in a manner dependent on EDS1 (Chini et al., 2004). These observations suggest that in addition to ETI, EDS1 seems to play a role in abiotic stress responses, making it plausible that EDS1 is one of the determinants for trade-off or synergy between biotic and abiotic stress response. Such intertwined roles of these defense regulators may reflect the degree of complexity in biotic-abiotic signaling crosstalk. Nonetheless, in the context where EDS1 is involved in salt and osmotic stress responses, this study indicates that WRKY18/WRKY40 attenuation of EDS1-mediated defense signaling prevents over-induction of defense responses to prioritize abiotic stress tolerance.

The CAMTA3 transcription factor has been shown to regulate genes shared between PTI and ETI, a portion of which is also induced under abiotic stress (Jacob et al., 2018), suggesting a role for CAMTA3 as an important mediator for PTI-ETI signaling convergence and possibly with abiotic stress signaling as well. The highly similar dual roles of CAMTA3 to that of WRKY18/WRKY40 in defense regulation, their involvement in salt stress regulation (Prasad et al., 2016) and their negative regulation on *EDS1* (Du et al., 2009) imply that CAMTA3 also regulates PTST in addition to WRKY18/WRKY40. However, my PTST assay on dominant-negative CAMTA3 mutant shows that CAMTA3 is not required for PTST (Figure 14). This strengthens specific requirements for WRKY18/WRKY40 in PTST.

Successful induction of PTST by MAMPs (Figure 4B) and the apparently similar mode of PROPEP3 processing during salt stress and bacteria elicitation (Figure 9B) led me to conceive a role for bacterial recognition in PTST. Veritably, non-pathogenic bacteria confer PTST in a manner dependent on PTI signaling and WRKY18/WRKY40 (Figure 15, Figure 16A). Non-pathogenic bacteria are often commensals in plant microbiota where they have a

mutualistic relationship with the host, and possess critical and discernible functions including directly influencing the host immunity (Durán et al., 2018; Oter et al., 2018). My findings point to a model in which the commensals undergo alterations or disintegration under salt stress, which provide a salt stress signal that is perceived by plant PRRs.

The mutualistic relationship between plants and their microbiota requires a delicate balance to maintain homeostasis within the microbiota, the loss of which can result in immune-activating dishomeostasis (Castrillo et al., 2017; Xin et al., 2016). Environmental changes including salt stress alter the homeostasis and structure of the plant microbiota (Naylor et al., 2017; Rath et al., 2019), which could lead to depletion or increased abundance of particular bacterial strains. Seeing that microbiota shifts and specific strains of the commensals could trigger or interfere with plants' PTI responses (Castrillo et al., 2017; Oter et al., 2018), salt-induced dishomeostasis in the microbiota could potentially lead to PTI and/or PTST in a biotic/abiotic context-dependent manner.

My work presents the possibility that active contribution of specific microbiota members that provide stress-adaptive functions to the host plant i.e. plant-growth promoting rhizobacteria, PGPR, is not always needed when plants acquire abiotic stress tolerance through their associations with microbes. In a given stress condition, plants may not always opt to re-shape its microbiota (by altering alpha-diversity and species richness), rather, depending on the context, plants may opt to sense and adapt to changes in their microbiota dynamics/homeostasis (by coping with microbes available at a given habitat). This is reflected in the successful PTST conferred by non-PGPR *Pst* DC3000 Δ*hrpS* (Figure 15), and further supported by heat-killed bacteria that are deprived of active or potentially beneficial metabolites/proteins that could contribute to PTST (Figure 16B-C), making it most likely that recognition of the residual MAMPs is sufficient to induce salt tolerance in the host plant.

However, it should not be ruled out that the salt stress might also affect bacterial physiology in ways that increase MAMPs availability for plants' recognition and/or reduce the expression of effector-mediated suppression of host PRR signaling, especially since environmental conditions have major influence on the adaptive traits of bacteria that are crucial for plant-microbe interactions (Müller et al., 2016).

CONCLUSION

Due to their sessile and slow migration nature, plants have developed complex mechanisms to adapt to the constrains they encounter in their habitat such as unavoidable soil salinity and pathogen outbreak, which could occur simultaneously. The nature of these stressors influences plants to either respond synergistically or in a trade-off. In this study, I present three main findings to address the knowledge gap in the crosstalk between defense activation and salt tolerance, and the biological implication of this crosstalk.

Firstly, I have uncovered a signaling pathway and mechanism underlying the positive relationship between PRR-mediated defense activation and salt stress tolerance. I show that salt stress engages PTI whereby salt damage induces PROPEPs production for PEPR-mediated PTI signaling activation. This improves the stability of WRKY18/WRKY40 proteins under salt stress to enable their attenuation of *EDS1* to confer salt/osmotic tolerance.

I further demonstrate that PRR-mediated defense activation (PTI) confers salt/osmotic tolerance but not EDS1-mediated defense activation (ETI), by using PTI- and ETI-inducing bacteria. I argue that WRKY18/WRKY40 transcription factors function as molecular switches to prevent the over-induction of defense responses to pilot between tolerance (PTST) or trade-off in defense activation and salt tolerance.

In the final section of this study, I propose a hypothesis whereby plants perceive changes in salinity levels by modulating PTI responses triggered by the commensals in their microbiota. In light of successful PTST conferred by MAMPs, non-pathogenic bacteria and heat-killed bacteria, and along with evidence from the published literature, I postulate that changes in soil salinity causes microbiota dishomeostasis that consequently trigger plants' PTI responses, which in the presence of salt stress results in PTST.

ACKNOWLEDGEMENTS

First and foremost, I would like to express my greatest gratitude to my supervisor, Dr. Yusuke Saijo for his guidance and continuous support throughout the undertaking of this study. His immense knowledge has tremendously helped me in advancing my research and writing up this thesis. Importantly, he showed me what good science really is, and his patience and motivation have shaped me to be a very passionate researcher.

I am also grateful to the members of my thesis committee, Dr. Keiji Nakajima and Dr. Toshiro Ito, for their insightful comments, encouragements and stimulating discussions that incented me to deepen my research.

I would like to take this opportunity to thank Dr. Kohji Yamada for initiating this study, our collaborators Dr. Hirotaka Ariga, Dr. Teruaki Taji and Dr. Keisuke Tanaka from the Tokyo University of Agriculture; Dr. Imre Somssich and Dr. Jane Parker from the Max Planck Institute for lending their scientific and technical expertise. Without their contributions, this study would have been incomplete.

I am also grateful towards the ex-members of the laboratory of Plant Immunity, Dr. Tadashi Fujiwara and Dr. Taishi Hirase, and the current members of the laboratory including Dr. Yuri Tajima for assisting in data analysis, and who never cease to attend to my queries. A special thank you goes to Dr. Kei Hiruma, who not only tirelessly provided advices with regards to my study, but also personal advices that helped cleared my doubts concerning my future career directions. My wishes also extend to my friends for accepting nothing less than excellence from me, for supporting me emotionally and proving a fun environment to work in.

Thank you from the bottom of my heart.

REFERENCES

1. Alonso, J., Stepanova, A., Leisse, T., Kim, C., Chen, H., Shinn, P., Stevenson, D., Zimmerman, J., Barajas, P., Cheuk, R., et al. (2003). Genome-wide insertional mutagenesis of Arabidopsis thaliana. Science (80-.). *301*, 653–657.
2. Ariga, H., Katori, T., Tsuchimatsu, T., Hirase, T., Tajima, Y., Parker, J., Alcázar, R., Koornneef, M., Hoekenga, O., Lipka, A., et al. (2017). NLR locus-mediated trade-off between abiotic and biotic stress adaptation in Arabidopsis. Nat. Plants *3*, 17072.
3. Aslam, S., Erbs, G., Morrissey, K., Newman, M., Chinchilla, D., Boller, T., Molinaro, A., Jackson, R., and Cooper, R. (2009). Microbe-associated molecular pattern (MAMP) signatures, synergy, size and charge: influences on perception or mobility and host defence responses. Mol. Plant Pathol. *10*, 375–387.
4. Bailey, T., and Machanick, P. (2012). Inferring direct DNA binding from ChIP-seq. Nucleic Acids Res. *40*, e128.
5. Bakshi, M., and Oelmüller, R. (2014). WRKY transcription factors jack of many trades in plants. Plant Signal. Behav. *9*, e27700.
6. Bartels, S., Lori, M., Mbengue, M., van Verk, M., Klauser, D., Hander, T., Böni, R., Robatzek, S., and Boller, T. (2013). The family of Peps and their precursors in Arabidopsis: differential expression and localization but similar induction of pattern-triggered immune responses. J. Exp. Bot. *64*, 5309–5321.
7. Bartsch, M., Gobbato, E., Bednarek, P., Debey, S., Schultze, J., Bautor, J., and Parker, J. (2006). Salicylic acid-independent ENHANCED DISEASE SUSCEPTIBILITY1 signaling in Arabidopsis immunity and cell death is regulated by the monooxygenase FMO1 and the Nudix hydrolase NUDT7. Plant Cell *18*, 1038–1051.
8. Bhandari, D.D., Lapin, D., Kracher, B., von Born, P., Bautor, J., Niefind, K., and Parker, J.E. (2019). An EDS1 heterodimer signalling surface enforces timely reprogramming of immunity genes in Arabidopsis. Nat. Commun. *10*, 772.
9. Bhaskara, G., Nguyen, T., and Verslues, P. (2012). Unique Drought Resistance Functions of the Highly ABA-Induced Clade A Protein Phosphatase 2Cs. PLANT Physiol. *160*, 379–395.
10. Birkenbihl, R.P., Kracher, B., Roccaro, M., and Somssich, I.E. (2016). Induced Genome-Wide Binding of Three Arabidopsis WRKY Transcription Factors during Early MAMP-Triggered Immunity. Plant Cell *29*, 20–38.
11. Boller, T., and Felix, G. (2009). A Renaissance of Elicitors: Perception of Microbe-Associated Molecular Patterns and Danger Signals by Pattern-Recognition Receptors. Annu. Rev. Plant Biol. *60*, 379–406.
12. Bolton, M. (2009). Primary metabolism and plant defense--fuel for the fire. Mol. Plant Microbe Interact. *22*, 487–497.
13. Brotman, Y., Landau, U., Pnini, S., Lisec, J., Balazadeh, S., Mueller-Roeber, B., Zilberstein, A., Willmitzer, L., Chet, I., and Viterbo, A. (2012). The LysM receptor-like kinase LysM RLK1 is required to activate defense and abiotic-stress responses induced by overexpression of fungal chitinases in Arabidopsis plants. Mol. Plant *5*, 1113–1124.
14. Busk, P., Jensen, A., and Pagès, M. (1997). Regulatory elements in vivo in the promoter of the abscisic acid responsive gene rab17 from maize. Plant J. *11*, 1285–1295.
15. Cao, Y., Liang, Y., Tanaka, K., Nguyen, C., Jedrzejczak, R., Joachimiak, A., and Stacey, G. (2014). The kinase LYK5 is a major chitin receptor in Arabidopsis and forms a chitin-induced complex with related kinase CERK1. Elife *3*, e03766.
16. Castrillo, G., Teixeira, P., Paredes, S., Law, T., de Lorenzo, L., Feltcher, M., Finkel, O., Breakfield, N., Mieczkowski, P., Jones, C., et al. (2017). Root microbiota drive direct integration of phosphate stress and immunity. Nature *543*, 513–518.
17. Chen, D., Cao, Y., Li, H., Kim, D., Ahsan, N., Thelen, J., and Stacey, G. (2017). Extracellular ATP elicits DORN1-mediated RBOHD phosphorylation to regulate

stomatal aperture. Nat. Commun. *8*, 2265.
18. Chen, H., Lai, Z., Shi, J., Xiao, Y., Chen, Z., and Xu, P. (2010). Roles of arabidopsis WRKY18, WRKY40 and WRKY60 transcription factors in plant responses to abscisic acid and abiotic stress. BMC Plant Biol. *10*, 281.
19. Chinchilla, D., Zipfel, C., Robatzek, S., Kemmerling, B., Nürnberger, T., Jones, J., Felix, G., and Boller, T. (2007). A flagellin-induced complex of the receptor FLS2 and BAK1 initiates plant defence. Nature *448*, 497–500.
20. Chini, A., Grant, J., Seki, M., Shinozaki, K., and Loake, G. (2004). Drought tolerance established by enhanced expression of the CC-NBS-LRR gene, ADR1, requires salicylic acid, EDS1 and ABI1. Plant J. *38*, 810–822.
21. Choi, H., Hong, J., Ha, J., Kang, J., and Kim, S. (2000). ABFs, a family of ABA-responsive element binding factors. J. Biol. Chem. *275*, 1723–1730.
22. Choi, W., Toyota, M., Kim, S., Hilleary, R., and Gilroy, S. (2014). Salt stress-induced Ca2+ waves are associated with rapid, long-distance root-to-shoot signaling in plants. Proc. Natl. Acad. Sci. *111*, 6497–6502.
23. Couton, D., and Zipfel, C. (2016). Regulation of pattern recognition receptor signalling in plants. Nat. Rev. Immunol. *16*, 537–552.
24. Cunnac, S., Lindeberg, M., and Collmer, A. (2009). Pseudomonas syringae type III secretion system effectors: repertoires in search of functions. Curr. Opin. Microbiol. *12*, 53–60.
25. Daami-Remadi, M., Souissi, A., Ben Oun, H., Mansour, M., and Nasraoui, B. (2009). Salinity effects on Fusarium wilt severity and tomato growth. Dyn. Soil, Dyn. Plant *3*, 61–69.
26. Davies, J. (2014). Annexin-Mediated Calcium Signalling in Plants. Planta *3*, 128–140.
27. Dodds, P.N., and Rathjen, J.P. (2010). Plant immunity: Towards an integrated view of plantĝ€" pathogen interactions. Nat. Rev. Genet. *11*, 539–548.
28. Du, L., Ali, G., Simons, K., Hou, J., Yang, T., Reddy, A., and Poovaiah, B. (2009). Ca(2+)/calmodulin regulates salicylic-acid-mediated plant immunity457. Nature *457*, 1153–1158.
29. Duan, M.R., Nan, J., Liang, Y.H., Mao, P., Lu, L., Li, L., Wei, C., Lai, L., Li, Y., and Su, X.D. (2007). DNA binding mechanism revealed by high resolution crystal structure of Arabidopsis thaliana WRKY1 protein. Nucleic Acids Res. *35*, 1145–1154.
30. Durán, P., Thiergart, T., Garrido-Oter, R., Agler, M., Kemen, E., Schulze-Lefert, P., and Hacquard, S. (2018). Microbial Interkingdom Interactions in Roots Promote Arabidopsis Survival. Cell *175*, 973–983.
31. Espinoza, C., Liang, Y., and Stacey, G. (2017). Chitin receptor CERK1 links salt stress and chitin-triggered innate immunity in Arabidopsis. Plant J. *89*, 984–995.
32. Feng, W., Kita, D., Peaucelle, A., Cartwright, H., Doan, V., Duan, Q., Liu, M., Maman, J., Steinhorst, L., Schmitz-Thom, I., et al. (2018). The FERONIA Receptor Kinase Maintains Cell-Wall Integrity during Salt Stress through Ca2+ Signaling. Curr. Biol. *28*, 666–675.
33. Fortmeier, R., and Schubert, S. (1995). Salt tolerance of maize (Zea mays L.): the role of sodium exclusion. Plant, Cell Environ. *19*, 1041–1047.
34. Fujita, Y., Fujita, M., Satoh, R., Maruyama, K., Parvez, M., Seki, M., Hiratsu, K., Ohme-Takagi, M., Shinozaki, K., and Yamaguchi-Shinozaki, K. (2005). AREB1 is a transcription activator of novel ABRE-dependent ABA signaling that enhances drought stress tolerance in Arabidopsis. Plant Cell *17*, 3470–3488.
35. Fujita, Y., Fujita, M., Shinozaki, K., and Yamaguchi-Shinozaki, K. (2011). ABA-mediated transcriptional regulation in response to osmotic stress in plants. J. Plant Res. *124*, 509–525.
36. Furihata, T., Maruyama, K., Fujita, Y., Umezawa, T., Yoshida, R., Shinozaki, K., and Yamaguchi-Shinozaki, K. (2006). Abscisic acid-dependent multisite phosphorylation regulates the activity of a transcription activator AREB1. Proc. Natl. Acad. Sci. *103*, 1988–93.
37. Gao, Y., Liu, J., Yang, F., Zhang, G., Wang, D., Zhang, L., Ou, Y., and Yao, Y. (2019). The WRKY transcription factor SlWRKY8 promotes resistance to pathogen infection and mediates drought and salt stress tolerance in Solanum lycopersicum. Physiol. Plant.

38. Geng, Y., Wu, R., Wee, C., Xie, F., Wei, X., Chan, P., Tham, C., Duan, L., and Dinneny, J. (2013). A spatio-temporal understanding of growth regulation during the salt stress response in Arabidopsis. Plant Cell *25*, 2132–2154.
39. Gómez-Gómez, L., Felix, G., and Boller, T. (1999). A single locus determines sensitivity to bacterial flagellin in Arabidopsis thaliana. Plant J. *18*, 277–284.
40. González-Guzmán, M., Apostolova, N., Bellés, J., Barrero, J., Piqueras, P., Ponce, M., Micol, J., Serrano, R., and Rodríguez, P. (2002). The short-chain alcohol dehydrogenase ABA2 catalyzes the conversion of xanthoxin to abscisic aldehyde. Plant Cell *14*, 1833–1846.
41. Guo, Y., Halfter, U., Ishitani, M., and Zhu, J. (2001). Molecular Characterization of Functional Domains in the Protein Kinase SOS2 That Is Required for Plant Salt Tolerance. Plant Cell *13*, 1383–99.
42. Guo, Y., Qiu, Q., Quintero, F., Pardo, J., Ohta, M., Zhang, C., Schumaker, K., and Zhu, J. (2004). Transgenic Evaluation of Activated Mutant Alleles of SOS2 Reveals a Critical Requirement for Its Kinase Activity and C-Terminal Regulatory Domain for Salt Tolerance in Arabidopsis thaliana. Plant Cell *16*, 435–49.
43. Gust, A.A., and Felix, G. (2014). Receptor like proteins associate with SOBIR1-type of adaptors to form bimolecular receptor kinases. Curr. Opin. Plant Biol. *21*, 104–111.
44. Halfter, U., Ishitani, M., and Zhu, J. (2000). The Arabidopsis SOS2 protein kinase physically interacts with and is activated by the calcium-binding protein SOS3. Proc. Natl. Acad. Sci. *97*, 3735–3740.
45. Hander, T., Fernández-Fernández, Á.D., Kumpf, R.P., Willems, P., Schatowitz, H., Rombaut, D., Staes, A., Nolf, J., Pottie, R., Yao, P., et al. (2019). Damage on plants activates Ca 2+ -dependent metacaspases for release of immunomodulatory peptides. Science (80-.). *363*.
46. Hatsugai, N., Igarashi, D., Mase, K., Lu, Y., Tsuda, Y., Chakravarthy, S., Wei, H., Foley, J., Collmer, A., Glazebrook, J., et al. (2017). A plant effector-triggered immunity signaling sector is inhibited by pattern-triggered immunity. EMBO J. *36*, 2758–2769.
47. Heese, A., Hann, D.R., Gimenez-Ibanez, S., Jones, A.M.E., He, K., Li, J., Schroeder, J.I., Peck, S.C., and Rathjen, J.P. (2007). The receptor-like kinase SERK3/BAK1 is a central regulator of innate immunity in plants. Proc. Natl. Acad. Sci. *104*, 12217–12222.
48. Huffaker, A., and Ryan, C.A. (2007). Endogenous peptide defense signals in Arabidopsis differentially amplify signaling for the innate immune response. Proc. Natl. Acad. Sci. *104*, 10732–10736.
49. Huot, B., Yao, J., Montgomery, B., and He, S. (2014). Growth-defense tradeoffs in plants: a balancing act to optimize fitnes. Mol. Plant *7*, 1267–1287.
50. Hütsch, B., Augustin, J., and Merbach, W. (2004). Plant rhizodeposition — an important source for carbon turnover in soils. J. Plant Nutr. Soil Sci. *165*, 397–407.
51. Ishitani, M., Liu, J., Halfter, U., Kim, C., Shi, W., and Zhu, J. (2000). SOS3 function in plant salt tolerance requires N-myristoylation and calcium binding. Plant Cell *12*, 667–678.
52. Jacob, F., Kracher, B., Mine, A., Seyfferth, C., Blanvillain-Baufumé, S., Parker, J., Tsuda, K., Schulze-Lefert, P., and Maekawa, T. (2018). A dominant-interfering camta3 mutation compromises primary transcriptional outputs mediated by both cell surface and intracellular immune receptors in Arabidopsis thaliana. New Phytol. *217*, 1667–1680.
53. Ji, H., Pardo, J., Batelli, G., Van Oosten, M., Bressan, R., and Li, X. (2013). The Salt Overly Sensitive (SOS) pathway: established and emerging roles. Mol. Plant *6*, 275–286.
54. Jiang, C., Belfield, E., Mithani, A., Visscher, A., Ragoussis, J., Mott, R., Smith, J., and Harberda, N. (2012). ROS-mediated vascular homeostatic control of root-to-shoot soil Na delivery in Arabidopsis. EMBO J. *31*, 4359–70.
55. Jiang, Z., Zhou, X., Tao, M., Yuan, F., Liu, L., Wu, F., Wu, X., Xiang, Y., Niu, Y., Liu, F., et al. (2019). Plant cell-surface GIPC sphingolipids sense salt to trigger Ca2+ influx. Nature *572*, 341–356.
56. Jones, J., and Dangl, J. (2006). The plant immune system. Nature *444*, 323–329.

57. Kadota, Y., Shirasu, K., and Zipfel, C. (2015). Regulation of the NADPH Oxidase RBOHD during Plant Immunity. Plant Cell Physiol. *56*, 1472–1480.
58. Karim, S., Lundh, D., Holmström, K., Mandal, A., and Pirhonen, M. (2005). Structural and functional characterization of AtPTR3, a stress-induced peptide transporter of Arabidopsis. J. Mol. Model. *11*, 226–236.
59. Karim, S., Holmström, K., Mandal, A., Dahl, P., Hohmann, S., Brader, G., Palva, E., and Pirhonen, M. (2007). AtPTR3, a wound-induced peptide transporter needed for defence against virulent bacterial pathogens in Arabidopsis. Planta *225*, 1431-45.
60. Katagiri, F., and Tsuda, K. (2010). Understanding the plant immune system. Mol. Plant Microbe Interact. *23*, 1531–1536.
61. Krol, E., Mentzel, T., Chinchilla, D., Boller, T., Felix, G., Kemmerling, B., Postel, S., Arents, M., Jeworutzki, E., Al-Rasheid, K., et al. (2010). Perception of the Arabidopsis danger signal peptide 1 involves the pattern recognition receptor AtPEPR1 and its close homologue AtPEPR2. J. Biol. Chem. *285*, 13471–13479.
62. Kunze, G. (2004). The N Terminus of Bacterial Elongation Factor Tu Elicits Innate Immunity in Arabidopsis Plants. Plant Cell *16*, 3496–3507.
63. Kusajima, M., Kwon, S., Nakajima, M., Sato, T., Yamakawa, T., Akutsu, K., and H, N. (2012). Induction of Systemic Acquired Resistance by Heat Shock Treatment in Arabidopsis. Biosci. Biotechnol. Biochem. *76*, 2301–2306.
64. Kushalappa, A.C., Yogendra, K.N., and Karre, S. (2016). Plant Innate Immune Response: Qualitative and Quantitative Resistance. CRC. Crit. Rev. Plant Sci. *35*, 38–55.
65. Lal, N.K., Nagalakshmi, U., Hurlburt, N.K., Flores, R., Bak, A., Sone, P., Ma, X., Song, G., Walley, J., Shan, L., et al. (2018). The Receptor-like Cytoplasmic Kinase BIK1 Localizes to the Nucleus and Regulates Defense Hormone Expression during Plant Innate Immunity. Cell Host Microbe *23*, 485-497.e5.
66. Lee, H.A., and Yeom, S.I. (2015). Plant NB-LRR proteins: Tightly regulated sensors in a complex manner. Brief. Funct. Genomics *14*, 233–242.
67. Léon-Kloosterziel, K., Gil, M., Ruijs, G., Jacobsen, S., Olszewski, N., Schwartz, S., Zeevaart, J., and Koornneef, M. (1996). Isolation and characterization of abscisic acid-deficient Arabidopsis mutants at two new loci. Plant J. *10*, 655–661.
68. Li, L., Li, M., Yu, L., Zhou, Z., Liang, X., Liu, Z., Cai, G., Gao, L., Zhang, X., Wang, Y., et al. (2014). The FLS2-associated kinase BIK1 directly phosphorylates the NADPH oxidase RbohD to control plant immunity. Cell Host Microbe *15*, 329–338.
69. Liu, J., and Zhu, J. (1998). A calcium sensor homolog required for plant salt tolerance. Science (80-.). *280*, 1943–1945.
70. Liu, J., Ishitani, M., Halfter, U., Kim, C., and Zhu, J. (2000). The Arabidopsis thaliana SOS2 gene encodes a protein kinase that is required for salt tolerance. Proc. Natl. Acad. Sci. *97*, 3730–3734.
71. Logemann, E., Birkenbihl, R., Ülker, B., and Somssich, I. (2006). An improved method for preparing Agrobacterium cells that simplifies the Arabidopsis transformation protocol. Plant Methods *2*, 16.
72. Lu, D., Wu, S., Gao, X., Zhang, Y., Shan, L., and He, P. (2010). A receptor-like cytoplasmic kinase, BIK1, associates with a flagellin receptor complex to initiate plant innate immunity. Proc. Natl. Acad. Sci. *107*, 496–501.
73. Lukasik, E., and Takken, F.L. (2009). STANDing strong, resistance proteins instigators of plant defence. Curr. Opin. Plant Biol. *12*, 427–436.
74. Ma, L., Zhang, H., Sun, L., Jiao, Y., Zhang, G., Miao, C., Hao, F., and Author information (2012). NADPH oxidase AtrbohD and AtrbohF function in ROS-dependent regulation of Na^+/K^+ homeostasis in Arabidopsis under salt stress. J. Exp. Bot. *63*, 305–317.
75. Ma, L., Ye, J., Yang, Y., Lin, H., Yue, L., Luo, J., Long, Y., Fu, H., Liu, X., Zhang, Y., et al. (2019). he SOS2-SCaBP8 Complex Generates and Fine-Tunes an AtANN4-Dependent Calcium Signature under Salt Stress. Dev. Cell *48*, 697–709.
76. Ma, X., Xu, G., He, P., and Shan, L. (2016). SERKing Coreceptors for Receptors. Trends Plant Sci. *21*, 1017–1033.
77. Meng, X., and Zhang, S. (2013). MAPK Cascades in Plant Disease Resistance Signaling. Annu. Rev. Phytopathol. *51*, 245–266.

78. Merlot, S., Gosti, F., Guerrier, D., Vavasseur, A., and Giraudat, J. (2011). The ABI1 and ABI2 protein phosphatases 2C act in a negative feedback regulatory loop of the abscisic acid signalling pathway. Plant J. *25*, 295–303.
79. Miller, W.T. (2009). Making Sense of Signal Transduction. Sci. Signal. *2*, pe79–pe79.
80. Miya, A., Albert, P., Shinya, T., Desaki, Y., Ichimura, K., Shirasu, K., Narusaka, Y., Kawakami, N., Kaku, H., and Shibuya, N. (2007). CERK1, a LysM receptor kinase, is essential for chitin elicitor signaling in Arabidopsis. Proc. Natl. Acad. Sci. *104*, 19613–18.
81. Müller, D., Vogel, C., Bai, Y., and Vorholt, J. (2016). The Plant Microbiota: Systems-Level Insights and Perspectives. Annu. Rev. Genet. *50*, 211–234.
82. Nakaminami, K., Okamoto, M., Higuchi-Takeuchi, M., Yoshizumi, T., Yamaguchi, Y., Fukao, Y., Shimizu, M., Ohashi, C., Tanaka, M., Matsui, M., et al. (2018). AtPep3 is a hormone-like peptide that plays a role in the salinity stress tolerance of plants. Proc. Natl. Acad. Sci. *115*, 5810–5815.
83. Navarro, L. (2004). The Transcriptional Innate Immune Response to flg22. Interplay and Overlap with Avr Gene-Dependent Defense Responses and Bacterial Pathogenesis. PLANT Physiol. *135*, 1113–1128.
84. Naylor, D., DeGraaf, S., Purdom, E., and Coleman-Derr, D. (2017). Drought and host selection influence bacterial community dynamics in the grass root microbiome. ISME J. *11*, 2681–2704.
85. Nejat, N., and Mantri, N. (2017). Plant Immune System: Crosstalk Between Responses to Biotic and Abiotic Stresses the Missing Link in Understanding Plant Defence. Curr. Issues Mol. Biol. *23*, 1–16.
86. Nekrasov, V., Li, J., Batoux, M., Roux, M., Chu, Z., Lacombe, S., Rougon, A., Bittel, P., Kiss-Papp, M., Chinchilla, D., et al. (2009). Control of the pattern-recognition receptor EFR by an ER protein complex in plant immunity. EMBO J. *28*, 3428–3438.
87. Nühse, T.S., Bottrill, A.R., Jones, A.M.E., and Peck, S.C. (2007). Quantitative phosphoproteomic analysis of plasma membrane proteins reveals regulatory mechanisms of plant innate immune responses. Plant J. *51*, 931–940.
88. Ohta, M., Guo =, Y., Halfter, U., and Zhu, J. (2003). A novel domain in the protein kinase SOS2 mediates interaction with the protein phosphatase 2C ABI2. Proc. Natl. Acad. Sci. *100*, 11771–6.
89. Orsini, F., Cascone, P., De Pascale, S., Barbieri, G., Corrado, G., Rao, R., and Maggio, A. (2009). Systemin-dependent salinity tolerance in tomato: evidence of specific convergence of abiotic and biotic stress responses. Physiol. Plant. *138*.
90. Oter, R., Nakano, R., Dombrowski, N., Ma, K., Team, A., McHardy, A., and Schulze-Lefert, P. (2018). Modular Traits of the Rhizobiales Root Microbiota and Their Evolutionary Relationship with Symbiotic Rhizobia. Cell Host Microbe *24*, 155–167.
91. Pandey, S.P., Roccaro, M., Schön, M., Logemann, E., and Somssich, I.E. (2010). Transcriptional reprogramming regulated by WRKY18 and WRKY40 facilitates powdery mildew infection of Arabidopsis. Plant J. *64*, 912–923.
92. Perraki, A., DeFalco, T.A., Derbyshire, P., Avila, J., Séré, D., Sklenar, J., Qi, X., Stransfeld, L., Schwessinger, B., Kadota, Y., et al. (2018). Phosphocode-dependent functional dichotomy of a common co-receptor in plant signalling. Nature *561*, 248–252.
93. Prasad, K., Abdel-Hameed, A., Xing, D., and Reddy, A. (2016). Global gene expression analysis using RNA-seq uncovered a new role for SR1/CAMTA3 transcription factor in salt stress. Sci. Rep. *6*, 27021.
94. Qiu, Q., Guo, Y., Dietrich, M., Schumaker, K., and Zhu, J. (2002). Regulation of SOS1, a plasma membrane Na+/H+ exchanger in Arabidopsis thaliana, by SOS2 and SOS3. Proc. Natl. Acad. Sci. *99*, 8436–41.
95. Quintero, F., Ohta, M., Shi, H., Zhu, J., and Pardo, M. (2002). Reconstitution in yeast of the Arabidopsis SOS signaling pathway for Na+ homeostasis. Proc. Natl. Acad. Sci. *99*, 9061–9066.
96. Raghavendra, A., Gonugunta, V., Christmann, A., and Grill, E. (2010). ABA perception and signalling. Trends Plant Sci. *15*, 395–401.
97. Ranf, S., Eschen-Lippold, L., Fröhlich, K., Westphal, L., Scheel, D., and Lee, J. (2014). Microbe-associated molecular pattern-induced calcium signaling requires the

receptor-like cytoplasmic kinases, PBL1 and BIK1. BMC Biol. *14*, 374.
98. Rath, K., Fierer, N., Murphy, D., and Rousk, J. (2019). Linking bacterial community composition to soil salinity along environmental gradients. ISME J. *13*, 836–846.
99. Rombauts, S., Florquin, K., Lescot, M., Marchal, K., Rouzé, P., and Van de Peer, Y. (2003). Computational Approaches to Identify Promoters and cis-Regulatory Elements in Plant Genomes. Plant Physiol. *132*, 1162–1176.
100. Ross, A., Yamada, K., Hiruma, K., Yamashita-Yamada, M., Lu, X., Takano, Y., Tsuda, K., and Saijo, Y. (2014). The Arabidopsis PEPR pathway couples local and systemic plant immunity. EMBO J. *33*, 61–75.
101. Roux, M., Schwessinger, B., Albrecht, C., Chinchilla, D., Jones, A., Holton, N., Malinovsky, F.G., Tör, M., de Vries, S., and Zipfel, C. (2011). The Arabidopsis Leucine-Rich Repeat Receptor–Like Kinases BAK1/SERK3 and BKK1/SERK4 Are Required for Innate Immunity to Hemibiotrophic and Biotrophic Pathogens . Plant Cell *23*, 2440–2455.
102. Rushton, P.J., Somssich, I.E., Ringler, P., and Shen, Q.J. (2010). WRKY transcription factors. Trends Plant Sci. *15*, 247–258.
103. Saijo, Y., Tintor, N., Lu, X., Rauf, P., Pajerowska-Mukhtar, K., Häweker, H., Dong, X., Robatzek, S., and Schulze-Lefert, P. (2009). Receptor quality control in the endoplasmic reticulum for plant innate immunity. EMBO J. *28*, 3439–3449.
104. Saijo, Y., Loo, E., and Yasuda, S. (2018). Pattern recognition receptors and signaling in plant-microbe interactions. Plant J. *93*, 591–613.
105. Sánchez-Barrena, M., Martínez-Ripoll, M., Zhu, J., and Albert, A. (2005). The structure of the Arabidopsis thaliana SOS3: molecular mechanism of sensing calcium for salt stress response. J. Mol. Biol. *345*, 1253–1264.
106. Schön, M., Töller, A., Diezel, C., Roth, C., Westphal, L., Wiermer, M., and Somssich, I.E. (2013). Analyses of wrky18 wrky40 Plants Reveal Critical Roles of SA/EDS1 Signaling and Indole-Glucosinolate Biosynthesis for Golovinomyces orontii Resistance and a Loss-of Resistance Towards Pseudomonas syringae pv. tomato AvrRPS4 . Mol. Plant-Microbe Interact. *26*, 758–767.
107. Schubert, S. (2014). Salt resistance of crop plants: physiological characterization of a multigenic trait (John Wiley & Sons, Inc).
108. Schwessinger, B., Roux, M., Kadota, Y., Ntoukakis, V., Sklenar, J., Jones, A., and Zipfel, C. (2011). Phosphorylation-dependent differential regulation of plant growth, cell death, and innate immunity by the regulatory receptor-like kinase BAK1. PLoS Genet. *7*.
109. Shabala, L., Cuin, T., Newman, I., and Shabala, S. (2005). Salinity-induced ion flux patterns from the excised roots of Arabidopsis sos mutants. Planta *222*, 1041–1050.
110. Shang, Y., Yan, L., Liu, Z., Cao, Z., Mei, C., Xin, Q., Wu, F., Wang, X., Du, S., Jiang, T., et al. (2010). The Mg-chelatase H subunit of Arabidopsis antagonizes a group of WRKY transcription repressors to relieve ABA-responsive genes of inhibition. Plant Cell *22*, 1909–1935.
111. Shen, Q., Saijo, Y., Mauch, S., Biskup, C., Bieri, S., Keller, B., Seki, H., Ulker, B., Somssich, I., and Schulze-Lefert, P. (2007). Nuclear activity of MLA immune receptors links isolate-specific and basal disease-resistance responses. Science (80-.). *315*, 1098–1103.
112. Shi, H., Ishitani, M., Kim, C., and Zhu, J. (2000). The Arabidopsis thaliana salt tolerance gene SOS1 encodes a putative Na+/H+ antiporter. Proc. Natl. Acad. Sci. *97*, 6896–901.
113. Stegmann, M., Monaghan, J., Smakowska-Luzan, E., Rovenich, H., Lehner, A., Holton, N., Belkhadir, Y., and Zipfel, C. (2017). The receptor kinase FER is a RALF-regulated scaffold controlling plant immune signaling. Science (80-.). *355*, 287–289.
114. Tanaka, K., Choi, J., Cao, C., and Stacey, G. (2014). Extracellular ATP acts as a damage-associated molecular pattern (DAMP) signal in plants. Front. Plant Sci. *5*, 446.
115. Tintor, N., Ross, A., Kanehara, K., Yamada, K., Fan, L., Kemmerling, B., Nürnberger, T., Tsuda, K., and Saijo, Y. (2013). Layered pattern receptor signaling via

ethylene and endogenous elicitor peptides during Arabidopsis immunity to bacterial infection. Proc. Natl. Acad. Sci. *110*, 6211–6216.
116. Torres, M.A., and Dangl, J.L. (2005). Functions of the respiratory burst oxidase in biotic interactions, abiotic stress and development. Curr. Opin. Plant Biol. *8*, 397–403.
117. Torres, M.A., Dangl, J.L., and Jones, J.D.G. (2002). Arabidopsis gp91phox homologues AtrbohD and AtrbohF are required for accumulation of reactive oxygen intermediates in the plant defense response. Proc. Natl. Acad. Sci. *99*, 517–522.
118. Tsuda, K., and Katagiri, F. (2010). Comparing signaling mechanisms engaged in pattern-triggered and effector-triggered immunity. Curr. Opin. Plant Biol. *13*, 459–465.
119. Veronese, P. (2005). The Membrane-Anchored BOTRYTIS-INDUCED KINASE1 Plays Distinct Roles in Arabidopsis Resistance to Necrotrophic and Biotrophic Pathogens. PLANT CELL ONLINE *18*, 257–273.
120. Wiermer, M., Feys, B., and Parker, J. (2005). Plant immunity: the EDS1 regulatory node. Curr. Opin. Plant Biol. *8*, 383–389.
121. Wu, S., Ding, L., and Zhu, J. (1996). SOS1, a Genetic Locus Essential for Salt Tolerance and Potassium Acquisition. Plant Cell *8*, 617–627.
122. Xiang, T., Zong, N., Zou, Y., Wu, Y., Zhang, J., Xing, W., Li, Y., Tang, X., Zhu, L., Chai, J., et al. (2008). Pseudomonas syringae Effector AvrPto Blocks Innate Immunity by Targeting Receptor Kinases. Curr. Biol. *18*, 74–80.
123. Xiao, Y., Stegmann, M., Han, Z., DeFalco, T., Parys, K., Xu, L., Belkhadir, Y., Zipfel, C., and Chai, J. (2019). Mechanisms of RALF peptide perception by a heterotypic receptor complex. Nature.
124. Xin, F., Nomura, K., Aung, K., Velásquez, A., Yao, J., Boutrot, F., Chang, J., Zipfel, C., and He, S. (2016). Bacteria establish an aqueous living space in plants crucial for virulence. Nature *539*, 524–529.
125. Xin, X.F., Kvitko, B., and He, S.Y. (2018). Pseudomonas syringae: What it takes to be a pathogen. Nat. Rev. Microbiol. *16*, 316–328.
126. Xu, X., Chen, C., Fan, B., and Chen, Z. (2006). Physical and Functional Interactions between Pathogen-Induced Arabidopsis WRKY18, WRKY40, and WRKY60 Transcription Factors. Plant Cell *18*, 1310–26.
127. Yamada, K., Yamashita-Yamada, M., Hirase, T., Fujiwara, T., Tsuda, K., Hiruma, K., and Saijo, Y. (2016). Danger peptide receptor signaling in plants ensures basal immunity upon pathogen-induced depletion of BAK1. EMBO J. *35*, 46–61.
128. Yamaguchi, Y., Pearce, G., and Ryan, C.A. (2006). The cell surface leucine-rich repeat receptor for AtPep1, an endogenous peptide elicitor in Arabidopsis, is functional in transgenic tobacco cells. Proc. Natl. Acad. Sci. *103*, 10104–10109.
129. Yamaguchi, Y., Huffaker, A., Bryan, A.C., Tax, F.E., and Ryan, C.A. (2010). PEPR2 is a second receptor for the Pep1 and Pep2 peptides and contributes to defense responses in Arabidopsis. Plant Cell *22*, 508–522.
130. Yan, L., Liu, Z., Xu, Y., Lu, K., and Wang, X. (2013). Auto- and Cross-repression of Three Arabidopsis WRKY Transcription Factors WRKY18, WRKY40, and WRKY60 Negatively Involved in ABA Signaling. J. Plant Growth Regul. *32*, 399–416.
131. Yang, H., Shi, Y., Liu, J., Guo, L., Zhang, X., and Yang, S. (2010). A mutant CHS3 protein with TIR-NB-LRR-LIM domains modulates growth, cell death and freezing tolerance in a temperature-dependent manner in Arabidopsis. Plant J. *63*, 283–296.
132. Yoshida, T., Fujita, Y., Maruyama K, Mogami, J., Todaka, D., Shinozaki, K., and Yamaguchi-Shinozaki, K. (2015). Four Arabidopsis AREB/ABF transcription factors function predominantly in gene expression downstream of SnRK2 kinases in abscisic acid signalling in response to osmotic stress. Plant, Cell Environ. *38*, 35–49.
133. Yu, L., Nie, J., Cao, C., Jin, Y., Yan, M., Wang, F., Liu, J., Xiao, Z., Liang, Y., and Zhang, W. (2010). Phosphatidic acid mediates salt stress response by regulation of MPK6 in Arabidopsis thaliana. New Phytol. *188*, 762–73.
134. Yu, X., Feng, B., He, P., and Shan, L. (2017). From Chaos to Harmony: Responses and Signaling upon Microbial Pattern Recognition. Annu. Rev.

Phytopathol. Is Online *55*, 109–146.
135. Yuan, F., Yang, H., Xue, Y., Kong, D., Ye, R., Li, C., Zhang, J., Theprungsirikul, L., Shrift, T., Krichilsky, B., et al. (2014). OSCA1 mediates osmotic-stress-evoked Ca2+ increases vital for osmosensing in Arabidopsis. Nature *514*, 367–371.
136. Zhang, J., Li, W., Xiang, T., Liu, Z., Laluk, K., Ding, X., Zou, Y., Gao, M., Zhang, X., Chen, S., et al. (2010). Receptor-like cytoplasmic kinases integrate signaling from multiple plant immune receptors and are targeted by a Pseudomonas syringae effector. Cell Host Microbe *7*, 290–301.
137. Zhang, W., Fraiture, M., Kolb, D., Löffelhardt, B., Desaki, Y., Boutrot, F., Tör, M., Zipfel, C., Gust, A., and Brunner, F. (2013). Arabidopsis receptor-like protein30 and receptor-like kinase suppressor of BIR1-1/EVERSHED mediate innate immunity to necrotrophic fungi. Plant Cell *25*, 4227–4241.
138. Zhao, C., Zayed, O., Yu, Z., Jiang, W., Zhu, P., Hsu, C., Zhang, L., Tao, W., Lozano-Duran, R., and Zhu, J. (2018). Leucine-rich repeat extensin proteins regulate plant salt tolerance in Arabidopsis. Proc. Natl. Acad. Sci. *115*, 13123–13128.
139. Zhu, J. (2000). Genetic analysis of plant salt tolerance using Arabidopsis. Plant Physiol. *124*, 941–948.
140. Zhu, J. (2003). Regulation of ion homeostasis under salt stress. Curr. Opin. Plant Biol. *6*, 441–445.
141. Zipfel, C., Robatzek, S., Navarro, L., Oakeley, E., Jones, J., Felix G, and Boller, T. (2004). Bacterial disease resistance in Arabidopsis through flagellin perception. Nature *428*, 764–767.
142. Zipfel, C., Kunze, G., Chinchilla, D., Caniard, A., Jones, J.D.G., Boller, T., and Felix, G. (2006). Perception of the Bacterial PAMP EF-Tu by the Receptor EFR Restricts Agrobacterium-Mediated Transformation. Cell *125*, 749–760.

SUPPLEMENTARY INFORMATION

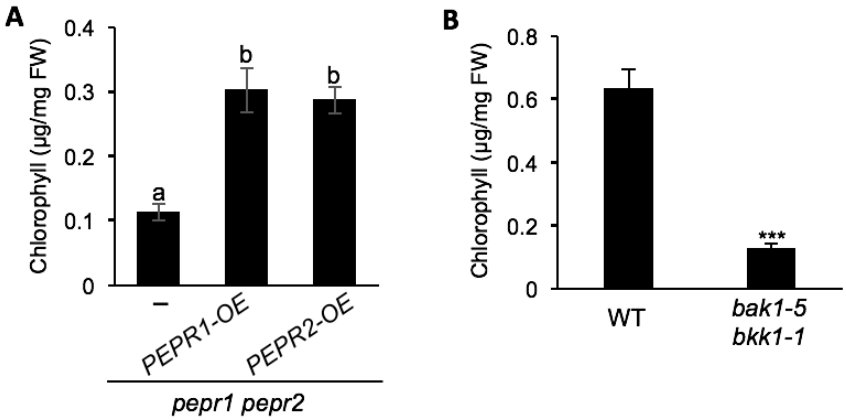

Supplementary Figure 1: PEPR signaling facilitates acquired osmotic tolerance
Quantification of chlorophyll contents in *pepr1 pepr2*, *PEPR1-OE*, *PEPR2-OE* (A), WT and *bak1-5 bkk1-1* (B) seedlings following 7 days of exposure to 100 mM NaCl and 14 days of exposure to osmotic stress with 750 mM sorbitol. Data from 4 biological replicates. Error bars indicate standard error. Letters above bars indicate $p < 0.05$ calculated with Tukey's HSD, ***$p < 0.001$ against WT, calculated using two-tailed t-test.